

Multi-Dimensional Unlimited Sampling and Robust Reconstruction

Dorian Florescu and Ayush Bhandari

Abstract

In this paper we introduce a new sampling and reconstruction approach for multi-dimensional analog signals. Building on top of the Unlimited Sensing Framework (USF), we present a new folded sampling operator called the multi-dimensional modulo-hysteresis that is also backwards compatible with the existing one-dimensional modulo operator. Unlike previous approaches, the proposed model is specifically tailored to multi-dimensional signals. In particular, the model uses certain redundancy in dimensions 2 and above, which is exploited for input recovery with robustness. We prove that the new operator is well-defined and its outputs have a bounded dynamic range. For the noiseless case, we derive a theoretically guaranteed input reconstruction approach. When the input is corrupted by Gaussian noise, we exploit redundancy in higher dimensions to provide a bound on the error probability and show this drops to 0 for high enough sampling rates leading to new theoretical guarantees for the noisy case. Our numerical examples corroborate the theoretical results and show that the proposed approach can handle a significantly larger amount of noise compared to USF.

Keywords: Analog-to-digital conversion, approximation, bandlimited functions, modulo sampling, Shannon sampling.

*D. Florescu and A. Bhandari are with the Department of Electrical and Electronic Engineering, Imperial College London, SW72AZ, UK. This work was supported by the UK Research and Innovation council's Future Leaders Fellowship program "Sensing Beyond Barriers" (MRC Fellowship award no. MR/S034897/1). E-mails: {D.Florescu, A.Bhandari}@imperial.ac.uk or ayush@alum.MIT.edu. Project page for (future) release of hardware design, code and data: <https://bit.ly/USF-Link>.

Contents

1	Introduction	3
1.1	Unlimited Sensing Framework (USF)	4
2	Modulo acquisition and recovery	9
2.1	Recovery from one-dimensional modulo data	9
3	Multi-dimensional modulo sampling	10
3.1	Multi-dimensional lattice sampling preliminaries	10
3.2	Previous approaches for recovery from multi-dimensional data	11
3.3	Towards multi-dimensional modulo-hysteresis acquisition	13
3.4	Properties of the proposed operator	15
3.5	Problem formulation	18
4	Detecting modulo-hysteresis discontinuities	19
4.1	Detecting folding times and signs	20
4.2	Detecting constants $M_{\mathbb{F}}$	22
5	Input reconstruction	23
5.1	Recovery with the proposed operator	23
5.2	Comparison to ideal modulo recovery with Gaussian noise measurements	24
6	Numerical study	26
7	Proofs	28
7.1	Multi-Dimensional Modulo Properties	28
7.2	Multi-Dimensional Modulo Recovery	35
8	Conclusion	42

1. Introduction

Shannon’s sampling theory is the workhorse of almost all modern-world digital systems. Its practical implementation is carried out via electronic hardware, namely, the analog-to-digital converter (ADC). However, there is a gap between theory and practice which leads to a few fundamental deviations from the ideal sampling model, including, among others, quantization (see the extensive survey by Gray & Neuhoff [1]) non-pointwise sampling [2] and ADC saturation. The latter deviation arises from the fact that the ADC is a physical device and hence, one can only record a fixed range of amplitudes (typically, a prescribed voltage range). This input amplitude range defines the *dynamic range* (or DR) of the ADC, say $\lambda > 0$. Any signal exceeding (in absolute value) λ would result in permanent loss of information due to saturation or clipping. Mathematically, this is synonymous to *hard thresholding* [3, 4], but the difference is that it occurs in hardware and is highly undesirable. Clipped sample values lead to high frequency components, which in turn leads to aliasing. Typical solutions to the saturation problem rely on:

- (a) hardware approaches such as *companding* [5] or adaptively matching the dynamic range to the input signal range via *automatic gain control*. There are also techniques that re-think ADC design (see, for example, [6]).
- (b) algorithmic approaches that aim to solve the inverse problem of *de-clipping* [7, 8] or *inpainting* [9].

Clipping or saturation is also highly relevant in the context of digital imaging, so much so that almost all modern smartphones are equipped with the *High Dynamic Range* or “HDR” mode, based on multiple captures that are combined numerically [10].

The progress in the last many decades has led to deepened understanding of the nuances involved with the quantization and limited DR aspects. Clearly, ADCs need to be matched to the DR of the input signal to avoid saturation or clipping. Beyond this calibration step—typically addressed by the engineers—there is an additional challenge: higher dynamic range requires a higher number of bits to achieve a given resolution; this in turn leads to a higher power consumption in the ADC, thus highlighting the

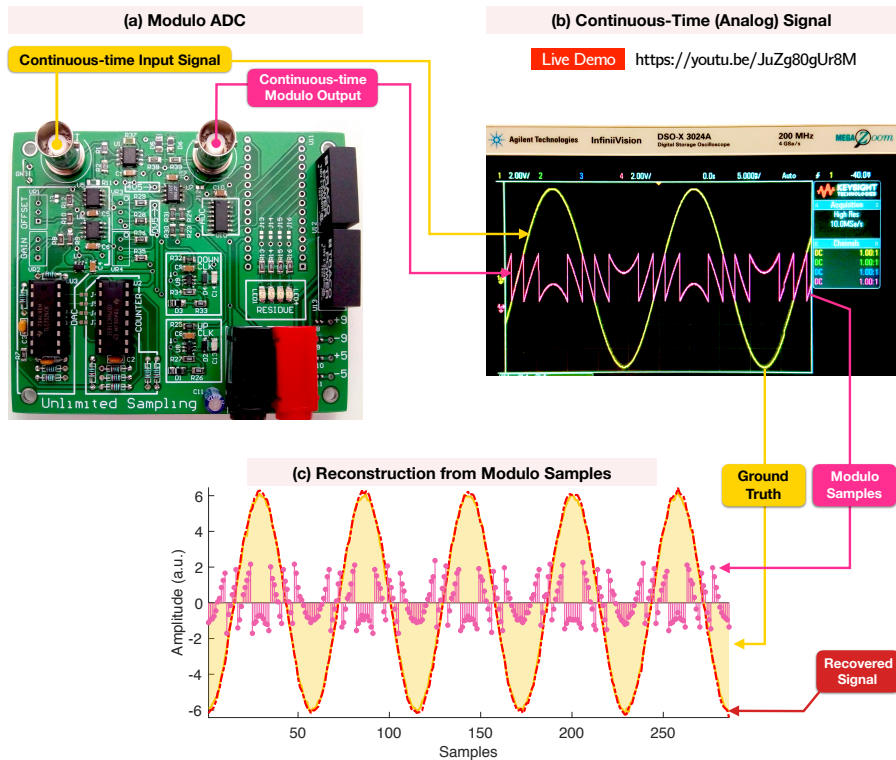


Figure 1: Signal acquisition and recovery pipeline for Unlimited Sensing Framework [11, 12]. (a) Modulo sampling hardware [13]. (b) Continuous-time signal waveforms on an oscilloscope. (c) Signal reconstruction using recovery algorithms [11, 12, 13, 14].

integral role of DR in digital acquisition.

1.1. Unlimited Sensing Framework (USF)

Recently, the Unlimited Sensing Framework (USF) [11, 15, 16, 17, 18, 12, 13] has been proposed in the literature that serves as an alternative digital acquisition protocol for avoiding the DR limitation in conventional ADCs. The USF is based on a joint design of hardware and mathematical algorithms.

- In hardware, the modulo non-linearity ensures that HDR inputs are folded back in to the ADC's DR; this is because the modulo threshold is chosen such that the modulo ADC's range is bounded by λ . Consequently, the modulo ADC results in *folded samples*.

- To recover the HDR input from folded, modulo samples, mathematically guaranteed recovery algorithms are deployed.

Similar to the Shannon–Nyquist sampling criterion where a higher input bandwidth can be traded off for higher sampling rates, it was shown that HDR signals can also be tackled by sampling more densely. This is made precise by the following theorem.

Theorem 1 (Unlimited Sampling Theorem [11]). *Let $f(t)$ be a continuous-time function with maximum frequency Ω (rads/s). Then, a sufficient condition for recovery of $f(t)$ from its modulo samples (up to an additive constant) taken every T seconds apart is $T \leq 1/(2\Omega e)$ where e is Euler’s number.*

Thus, the USF addresses a major bottleneck in physical sensors by allowing the recovery of inputs beyond the sensor dynamic range. A first validation of the USF with experiments based on a modulo ADC were presented in [13]. In particular, it was shown that signals as large as $\approx 25\lambda$ can be recovered in a laboratory setup. The full sampling and reconstruction pipeline for the USF is shown in Fig. 1.

The initial works based on USF tackled signals supported on the real line spanned in a bandlimited [11, 12] or spline spaces [19]. There are also methods to recover signals with compressive priors [20, 21] and using wavelet filters [22]. Further extensions of the USF include compactly supported inputs [13], sparse signals [23] and also new acquisition models [14].

A new acquisition model called modulo-hysteresis was introduced in [24] and further discussed in [14], which considers hardware non-idealities and enables new recovery guarantees. The modulo-hysteresis was also implemented in a hardware prototype [14]. This line of work also paved the path to novel and exciting low-power acquisition neuromorphic applications [24, 25].

The methods discussed so far assume that the input is one-dimensional. However, in many applications, such as photography [19], X-ray imaging or Computed Tomography [26], the input signal is multi-dimensional.

Motivation for a multi-dimensional model. There have been attempts to address multi-dimensional inputs with modulo architectures by rasterizing and processing the signal

line-by-line in imaging [27, 19, 26] or for lattice sampling [28]. However, the existing modulo sampling approaches for multi-dimensional data are based on a one-dimensional modulo operator that is applied sequentially on the slices of a multi-dimensional input. This considers each slice a distinct signal, and does not exploit that they are all part of a multi-dimensional input. In other words, this modulo operation represents a separable transformation that does not exploit the multi-dimensional nature of the input. Furthermore, it is known that non-separable transformations represent much more powerful tools in analysing multi-dimensional data [29, 30].

We consider only the problem of input recovery for noisy inputs, distinct from that of input denoising, which was addressed before for modulo sampling [31, 32]. Methods such as USF recover the noise corrupted input samples while keeping the noise sequence intact. However, USF (Theorem 1) is fundamentally restricted to work with noise amplitudes smaller than the modulo threshold. When this requirement is not satisfied, the input recovery is heavily distorted. This limitation is carried over to the existing attempts to apply USF to multi-dimensional data.

Contributions. Here we present a modulo model that exploits the multi-dimensional structure of the data in the encoding process. Specifically, via multi-dimensional sampling in D dimensions, we are able to dedicate a $D - 1$ -dimensional subspace to deal with noise reduction, leaving dimension $d = 1$ for estimating the modulo folds. Specifically, our contributions are below:

- C₁) We introduce a generalized D -dimensional modulo operator for sampling on a lattice.
- C₂) We prove that the operator is well-defined and the folding discontinuities are located along directions given by the lattice vectors.
- C₃) We provide recovery guarantees under noiseless assumption.
- C₄) Under Gaussian noise assumption, we provide an upper bound on the recovery error probability that drops to 0 for high enough sampling rates.
- C₅) Using a numerical study we show that the proposed model offers significantly better noise robustness than USF.

Notation. For $x \in \mathbb{R}$, $\llbracket x \rrbracket = x - \lfloor x \rfloor$ denotes the fractional part of x and $\lfloor x \rfloor$ is the floor function. For a set \mathbb{S} , $\mathbb{1}_{\mathbb{S}}$ is the indicator function and $\text{cl}(\mathbb{S})$ is the set closure. The set of real and integer numbers are \mathbb{R} and \mathbb{Z} , respectively. Let $\mathbb{R}^* = \mathbb{R} \setminus \{0\}$ and $\mathbb{Z}^* = \mathbb{Z} \setminus \{0\}$, and let the sets restricted to positive numbers $x \geq 0$ be \mathbb{R}_+ and \mathbb{Z}_+ . We denote by \emptyset the empty set.

We use bold lowercase for vectors such as $\mathbf{x} = [x_1, \dots, x_D]^\top$, assumed to be column vectors unless otherwise specified. Matrices are denoted by bold uppercase, e.g., $\mathbf{M} \in \mathbb{R}^{D \times D}$. The element on line k_1 and column k_2 in matrix \mathbf{M} is denoted by $[\mathbf{M}]_{k_1, k_2}$. Unless specified otherwise, we use notation \mathbf{x} to denote a vector $\mathbf{x} \in \mathbb{Z}^D$ and $\bar{\mathbf{x}}$ to denote a vector $\bar{\mathbf{x}} \in \mathbb{Z}^{D-1}$. When used in the same context, $\bar{\mathbf{x}}$ denotes the last $D - 1$ coordinates of \mathbf{x} such that $\mathbf{x} = [x_1, \bar{\mathbf{x}}]$. Similarly, we denote by $\bar{\mathbf{V}} \in \mathbb{R}^{D \times (D-1)}$ a matrix containing the last $D - 1$ columns of matrix $\mathbf{V} \in \mathbb{R}^{D \times D}$. For two vectors $\mathbf{v}_1, \mathbf{v}_2 \in \mathbb{R}^D$ we denote their inner product by $\langle \mathbf{v}_1, \mathbf{v}_2 \rangle = \sum_{d=1}^D v_{1,d} \cdot \text{conj}(v_{2,d}) = \mathbf{v}_1^\top \cdot \text{conj}(\mathbf{v}_2)$, where conj is the complex-conjugate. Norm $\|\mathbf{v}\|_2$ denotes the Euclidean norm for a vector $\mathbf{v} \in \mathbb{R}^D$ and norm $\|\mathbf{v}\|_\infty$ is defined as $\|\mathbf{v}\|_\infty = \max_{d=1, \dots, D} |[\mathbf{v}]_d|$. We denote by $\det(\mathbf{V})$ the determinant of matrix \mathbf{V} . We denote by $\mathbf{T} = \text{diag}\{T_1, \dots, T_D\}$ a matrix with T_1, \dots, T_D on the main diagonal and 0 otherwise.

For a function $f : \mathbb{R}^D \rightarrow \mathbb{R}$, $\|f\|_2$ and $\|f\|_\infty$ represent the $L^2(\mathbb{R}^D)$ and $L^\infty(\mathbb{R}^D)$ norms, respectively. We denote by $\mathcal{F}f$ the Fourier transform applied to f , defined as

$$\mathcal{F}f(\boldsymbol{\omega}) = \int_{\mathbb{R}^D} f(\mathbf{x}) e^{-j\langle \boldsymbol{\omega}, \mathbf{x} \rangle} d\mathbf{x}, \quad (1)$$

where $\mathbf{x} = [x_1, \dots, x_D]^\top$ and $\boldsymbol{\omega} = [\omega_1, \dots, \omega_D]^\top$. The inverse Fourier transform $\mathcal{F}^{-1}F$ is defined as

$$\mathcal{F}^{-1}F(\mathbf{x}) = \frac{1}{(2\pi)^D} \int_{\mathbb{R}^D} F(\boldsymbol{\omega}) e^{j\langle \boldsymbol{\omega}, \mathbf{x} \rangle} d\boldsymbol{\omega}. \quad (2)$$

The support of sequence ψ is denoted by $\text{supp}(\psi)$ and the support of a function $f(\mathbf{x})$ is $\text{supp}(f)$. For two multi-dimensional sequences $\gamma_1, \gamma_2 : \mathbb{Z}^D \rightarrow \mathbb{R}$, $\langle \gamma_1, \gamma_2 \rangle$ denotes the multi-dimensional inner product defined as $\langle \gamma_1, \gamma_2 \rangle = \sum_{\mathbf{k} \in \mathbb{Z}^D} \gamma_1[\mathbf{k}] \text{conj}(\gamma_2[\mathbf{k}])$. The coefficients for the forward finite difference of order N are denoted by $\Delta^N[k]$. Specifically, it is defined as $\Delta^N[k] = \Delta_-^N[-k]$, where Δ_-^N is defined recursively as

$\Delta_-^{N+1}[k] = \Delta_-^N * \Delta_-^1[k]$, where $\Delta_-^1[-1] = 1, \Delta_-^1[0] = -1, \Delta_-^1[k] = 0, k \in \mathbb{Z} \setminus \{-1, 1\}$.

We denote by $\mathbf{v}_1, \dots, \mathbf{v}_D$ the set of vectors defining a lattice $\Lambda = \{\mathbf{V}\mathbf{T}\mathbf{k}, \mathbf{k} \in \mathbb{Z}^D\}$ where $\mathbf{V} = [\mathbf{v}_1, \dots, \mathbf{v}_D], \mathbf{v}_d \in \mathbb{R}^D, \forall d \in \{1, \dots, D\}$ and $\mathbf{T} = \text{diag}\{T_1, \dots, T_D\}$, where T_d denotes the sampling period across dimension $d \in \{1, \dots, D\}$. Without loss of generality, we assume that \mathbf{v}_d are *versors*, i.e., $\|\mathbf{v}_d\|_2 = 1, \forall d \in \{1, \dots, D\}$. The vectors are assumed linearly independent, and thus \mathbf{V} is invertible. Therefore, a function $f : \mathbb{R}^D \rightarrow \mathbb{R}$ can be equivalently evaluated using Cartesian coordinates as $f(\mathbf{x}_c)$ or lattice coordinates as $f(\mathbf{V}\mathbf{x}_v)$ such that $\mathbf{x}_v = \mathbf{V}^{-1}\mathbf{x}_c$. Unless specified otherwise, $\gamma[\mathbf{k}], \mathbf{k} \in \mathbb{Z}^D$, denote the samples of the input function f on lattice Λ such that $\gamma[\mathbf{k}] = f(\mathbf{V}\mathbf{T}\mathbf{k})$. The dual lattice $\hat{\Lambda}$ is defined as $\hat{\Lambda} = \{\hat{\mathbf{V}}\mathbf{T}^{-1}\mathbf{k} | \mathbf{k} \in \mathbb{Z}^D\}$, where $\hat{\mathbf{V}} = \mathbf{V}^{-\top} = (\mathbf{V}^{-1})^\top$ and $\mathbf{T}^{-1} = \text{diag}\{1/T_1, \dots, 1/T_D\}$.

The D -dimensional Paley-Wiener space $\text{PW}_\Omega(\mathbb{R}^D)$ of bandwidth Ω relative to lattice Λ consists of functions $f \in L^2(\mathbb{R}^D)$ such that

$$\text{supp}(\mathcal{F}f) \subseteq \left\{ \hat{\mathbf{V}}\boldsymbol{\omega} = \sum_{d=1}^D \omega_d \hat{v}_d \in \mathbb{R}^D \mid |\omega_d| < \Omega_d, \forall d \in \{1, \dots, D\} \right\}. \quad (3)$$

For the one-dimensional case $D = 1$, the lattice matrices $\hat{\mathbf{V}}$ reduce to the trivial case $\hat{\mathbf{V}} = \mathbf{V} = [1]$ and $\text{PW}_\Omega(\mathbb{R}^D)$ reduces to the classical one-dimensional Paley-Wiener space $\text{PW}_\Omega(\mathbb{R})$.

For a random variable η we denote by p.d.f. its probability density function. We denote by $\mathcal{N}(\mu, \sigma^2)$ the normal distribution with mean μ and standard deviation σ . A random variable η drawn from the Gaussian normal distribution is denoted as $\eta \sim \mathcal{N}(\mu, \sigma^2)$.

2. Modulo acquisition and recovery

2.1. Recovery from one-dimensional modulo data

The centered modulo with threshold λ is a function $\mathcal{M}_\lambda : \mathbb{R} \rightarrow \mathbb{R}$ satisfying [12]

$$\mathcal{M}_\lambda(x) = 2\lambda \left(\left\lfloor \frac{x}{2\lambda} + \frac{1}{2} \right\rfloor - \frac{1}{2} \right). \quad (4)$$

When applied to a one-dimensional function g the modulo non-linearity generates values $\mathcal{M}_\lambda(g(t)) \in [-\lambda, \lambda]$.

In analogy to Shannon-Nyquist sampling theory, the first recovery result in the Unlimited Sensing Framework (USF) utilized bandlimited inputs, namely, $g \in \text{PW}_\Omega$. In the noiseless scenario, the *unlimited sampling theorem* [11, 12] guarantees that the input of the ideal modulo encoder can be recovered from the output samples provided that the sampling period satisfies $T < \frac{1}{2\Omega e}$. Furthermore, reconstruction is also possible in the case of data corrupted by bounded noise if the following is true [12]

$$(T\Omega e)^N g_\infty + 2^N \eta_\infty < \lambda. \quad (5)$$

The recovery approach used in [11, 12] aims to reconstruct the residual function $\varepsilon_g(t)$ defined as $\varepsilon_g(t) \triangleq g(t) - \mathcal{M}_\lambda(g(t)) \in 2\lambda \cdot \mathbb{Z}$. In other words, for the ideal modulo encoder the values of $\varepsilon_g(t)$ lie on an equally spaced grid with step 2λ . However, this is not true for non-ideal modulo encoders exhibiting phenomena such as hysteresis, leading to reconstruction distortions.

A generalized model of the modulo operator, called *modulo-hysteresis*, was introduced for the one-dimensional scenario [33, 34, 14]. Here, we generalize this model to multi-dimensional sampling. As in the one-dimensional case, we will show that modulo-hysteresis enables the separation of the folding times, which will be used in the recovery in Section 3, 4, and 5. We begin with the definition of the one-dimensional modulo-hysteresis.

Definition 1 (One-dimensional modulo-hysteresis). *The operator \mathcal{M}_H with threshold λ and hysteresis $h \in [0, 2\lambda/3)$, where $H = \lfloor \lambda h \rfloor$, generates a function $z(t) = \mathcal{M}_H g(t)$ for input $g \in \text{PW}_\Omega(\mathbb{R})$, such that, for $t \geq 0$*

$$z(t) = g(t) - \varepsilon_g(t), \quad (6)$$

where

- $\varepsilon_g(t) = 2\lambda_h \sum_{r=1}^R s_r \mathbf{1}_{[\tau_r, \infty)}(t) + hM$, $\lambda_h \triangleq \lambda - h/2$,
- $M = \left\lfloor \frac{g(0)+\lambda}{h} \right\rfloor - 1$,
- τ_r and s_r are the folding time and sign respectively, satisfying $\tau_0 = s_0 = 0$ and

$$\begin{aligned} \tau_1 &= \inf \{t > \tau_0 \mid \mathcal{M}_\lambda(g(t) + \lambda) = 0\}, \\ s_r &= \text{sign}(g(\tau_r) - g(\tau_{r-1})), \\ \tau_{r+1} &= \inf \{t > \tau_r \mid \mathcal{M}_\lambda(g(t) - g(\tau_r) + hs_r) = 0\}, \quad r \geq 1. \end{aligned} \quad (7)$$

Furthermore, for $t < 0$ we have $z(t) = \mathcal{M}_\mathbf{H}[g(-\cdot)](-t)$. Let $\tau_r^-, s_r^-, r \geq 1$ be the sequence of folding times and signs computed via (7) for $\mathcal{M}_\mathbf{H}[g(-\cdot)]$. Then we define $\tau_r \triangleq -\tau_{-r}^-, s_r \triangleq s_{-r}^-, r \in \mathbb{Z}, r < 0$.

A key property of the 1D modulo-hysteresis is the folding time separation [14, 33]

$$\tau_{r+1} - \tau_r \geq \frac{h}{\Omega \|g\|_\infty}. \quad (8)$$

We note that the ideal modulo, which satisfies $\mathcal{M}_\lambda(g(t)) = \mathcal{M}_\mathbf{H}g(t)$ for $h = 0$ does not guarantee any separation via (8). The reconstruction problem proposed aims to recover $g(kT)$ from $y[k] = z(kT)$. Furthermore, it was shown that this approach enables handling a number of modulo non-idealities [14, 35, 33, 24].

3. Multi-dimensional modulo sampling

3.1. Multi-dimensional lattice sampling preliminaries

Let $f : \mathbb{R}^D \rightarrow \mathbb{R}$ be a D -dimensional scalar function. The data is then sampled on a lattice $\Lambda = \{\mathbf{V}\mathbf{T}\mathbf{k} \mid \mathbf{k} \in \mathbb{Z}^D\}$. We denote the resulting samples by $\gamma[\mathbf{k}] = f(\mathbf{V}\mathbf{T}\mathbf{k})$. We assume that f has a Fourier transform satisfying

$$\text{supp}(\mathcal{F}f) \subseteq \mathbb{D}.$$

Upon sampling, the spectrum of f is copied periodically, to produce the multi-dimensional discrete-time Fourier transform $F_{\Lambda}(\boldsymbol{\omega}) = \sum_{\mathbf{k} \in \mathbb{Z}^D} f(\mathbf{V}\mathbf{T}\mathbf{k}) e^{-j\langle \boldsymbol{\omega}, \mathbf{k} \rangle}$, whose support satisfies

$$\text{supp}(F_{\Lambda}) = \mathbf{T}\mathbf{V}^{\top} \cdot \bigcup_{\mathbf{n} \in \widehat{\Lambda}} (\mathbb{D} + 2\pi\mathbf{n}). \quad (9)$$

It was shown that f can be recovered from its lattice samples $\gamma[\mathbf{k}]$ if [36, 37]

$$\mathbf{T}\mathbf{V}^{\top}(\mathbb{D} + 2\pi\mathbf{n}_1) \cap \mathbf{T}\mathbf{V}^{\top}(\mathbb{D} + 2\pi\mathbf{n}_2) = \emptyset, \quad \forall \mathbf{n}_1, \mathbf{n}_2 \in \widehat{\Lambda}, \mathbf{n}_1 \neq \mathbf{n}_2. \quad (10)$$

To ensure that recovery is possible, we assume that the spectrum of f has a compact support satisfying $\mathbb{D} \subseteq \widehat{\mathbf{V}} \prod_{d=1}^D (-\Omega_d, \Omega_d)$. Formally, our assumption is $f \in \text{PW}_{\Omega}(\mathbb{R}^D)$. Then f can be reconstructed from samples $\gamma[\mathbf{k}]$ if (10) is satisfied, which is sufficiently guaranteed if we replace \mathbb{D} by $\widehat{\mathbf{V}} \cdot \prod_{d=1}^D (-\Omega_d, \Omega_d)$, for which the terms on the left-hand-side of (10) are computed as

$$\mathbf{T}\mathbf{V}^{\top}(\mathbb{D} + 2\pi\mathbf{n}) = \mathbf{T}\mathbf{V}^{\top} \left[\mathbf{V}^{-\top} \prod_{d=1}^D (-\Omega_d, \Omega_d) + 2\pi\mathbf{n} \right], \quad \mathbf{n} \in \widehat{\Lambda}. \quad (11)$$

We use that $\mathbf{n} = \mathbf{V}^{-\top} \mathbf{T}^{-1} \mathbf{k}$, $\mathbf{k} \in \mathbb{Z}^D$, yielding

$$\mathbf{T}\mathbf{V}^{\top}(\mathbb{D} + 2\pi\mathbf{n}) = \mathbf{T} \prod_{d=1}^D (-\Omega_d, \Omega_d) + 2\pi\mathbf{k}, \quad \mathbf{k} \in \mathbb{Z}^D \quad (12)$$

$$= \prod_{d=1}^D (-T_d\Omega_d, T_d\Omega_d) + 2\pi\mathbf{k}. \quad (13)$$

Therefore, (10) is true if

$$T_d < \frac{\pi}{\Omega_d}, \quad \forall d \in \{1, \dots, D\}. \quad (14)$$

Just as in the one-dimensional case, considering the problem of sensor saturation motivates using the concept of modulo folding also in the multi-dimensional case. Next we go through some of the attempts to apply modulo for multi-dimensional data.

3.2. Previous approaches for recovery from multi-dimensional data

As in the one-dimensional case, the problem with computing directly $\gamma[\mathbf{k}]$ is that the sample values may be very large which would saturate an analog-to-digital (ADC)

acquisition device, which has a restricted dynamic range [12]. The modulo operator was applied previously for multi-dimensional inputs by processing a 1D slice at a time [19, 28]. However, these methods are not truly multi-dimensional because they don't exploit the multi-dimensional structure of the data. Furthermore, when dealing with noise in 1D, the modulo samples $y[\mathbf{k}] = \gamma[\mathbf{k}] + \eta[\mathbf{k}] - \varepsilon_\gamma[\mathbf{k}]$ require the separation of both residual ε_γ and η within the same dimension. This turns out to be contradictory, as detecting ε_γ requires a high-pass filter (such as Δ^N in the case of USF), while denoising is typically done with low-pass filters [34]. Furthermore, a denoising approach on modulo data was tested for multi-dimensional signals [31]. However, we center our analysis on purely modulo inversion techniques, where the noise sequence remains unaltered.

We define the following functions, representing slices of function $f(\mathbf{V}\mathbf{x})$. Let $f_{\mathbf{V}}(\mathbf{x}) \triangleq f(\mathbf{V}\mathbf{x})$. Let $f_{\bar{\mathbf{x}}} : \mathbb{R} \rightarrow \mathbb{R}$ denote the slice along dimension x_1 defined as $f_{\bar{\mathbf{x}}}(x) \triangleq f\left(x\mathbf{v}_1 + \sum_{d=2}^D x_d \mathbf{v}_d\right)$, $\forall \bar{\mathbf{x}} \in \mathbb{R}^{D-1}$, $\bar{\mathbf{x}} = [x_2, \dots, x_D]$. In the next proposition we also use a generic slices defined as the one-dimensional function $g_d(x_d) \triangleq f\left(\sum_{n=1}^D x_n \mathbf{v}_n\right)$ by fixing dimensions $\{x_1, \dots, x_{d-1}, x_{d+1}, \dots, x_D\}$, $d \neq 1$. The following proposition was proven in [28].

Proposition 1 (Bandlimited slices). *The function $f_{\bar{\mathbf{x}}}$ satisfies $f_{\bar{\mathbf{x}}} \in \text{PW}_{\Omega_1}(\mathbb{R})$. Furthermore, $g_d \in \text{PW}_{\Omega_d}(\mathbb{R})$, $\forall d \in \{1, \dots, D\}$, $d \neq 1$.*

Proof. The proof is in Section 7.1. □

The proposition above proves that any *slice* of the multi-dimensional function f along lattice dimension d has the spectrum compactly supported within $(-\Omega_d, \Omega_d)$. Furthermore, this implies that a Bernštein bound can be applied for each variable such that

$$\begin{aligned} \left| \frac{\partial}{\partial x_d} f_{\mathbf{V}}(\mathbf{x}) \right| &\leq \Omega_d \max_{x_d} |f_{\mathbf{V}}(\mathbf{x})| \leq \Omega_d \|f_{\mathbf{V}}\|_\infty \\ &= \Omega_d \|f\|_\infty, \quad \forall d \in \{1, \dots, D\}, \forall \bar{\mathbf{x}} \in \mathbb{R}^{D-1}. \end{aligned} \tag{15}$$

The works in [19] and [28] apply one-dimensional ideal modulo to $f_{\bar{\mathbf{x}}}$:

$$\mathcal{M}_\lambda f_{\bar{\mathbf{x}}}(x) = f_{\bar{\mathbf{x}}}(x) - 2\lambda_h \sum_{r \in \mathbb{Z}} s_{\bar{\mathbf{x}}, r} \mathbb{1}_{[\tau_{\bar{\mathbf{x}}, r}, \infty)}(x), x \in \mathbb{R}.$$

Therefore we can define the "folded" multi-dimensional function $z(\mathbf{x})$ as

$$z(\mathbf{V}\mathbf{x}) = \mathcal{M}_\lambda(f_{\bar{\mathbf{x}}}(x_1)), \quad (16)$$

where $\mathbf{x} = [x_1, \dots, x_D]$, $\bar{\mathbf{x}} = [x_2, \dots, x_D]$, $x_d \in \mathbb{R}, \forall d \in \{1, \dots, D\}$. Subsequently, the output samples are $z(\mathbf{V}\mathbf{T}\mathbf{k}) = \mathcal{M}_\lambda f_{\bar{\mathbf{T}}\bar{\mathbf{k}}}(k_1 T_1)$, where $\bar{\mathbf{T}} = \text{diag}\{T_2, \dots, T_D\}$.

Then, recovering $f_{\bar{\mathbf{T}}\bar{\mathbf{k}}}(k_1 T_1)$ for all $\bar{\mathbf{T}}\bar{\mathbf{k}}$ from $z(\mathbf{V}\mathbf{T}\mathbf{k})$ represents a line-by-line approach used in [19, 26, 28], which is guaranteed to work if (5) holds true. However, as explained previously, this approach does not exploit the multi-dimensional structure of the input data. This is further motivated by the accepted knowledge in image processing that non-separability in multiple dimensions has a lot more to offer than separability [29, 30]. This motivates introducing a multi-dimensional modulo-hysteresis model in the next section. We will show that the new model allows a significantly large amount of noise, which is not possible with USF that processes the data line-by-line.

3.3. Towards multi-dimensional modulo-hysteresis acquisition

Inspired from the 1D modulo-hysteresis operator that showed improvements for noise robustness [34], we define in the following a new operator called multi-dimensional modulo-hysteresis that addresses the issues discussed in the previous subsection. The idea is to split the domain \mathbb{R}^{D-1} in disjoint sets confined in polytopes $\mathcal{P}_{\bar{\mathbf{b}}}$, $\bar{\mathbf{b}} \in \mathbb{Z}^{D-1}$ defined as

$$\mathcal{P}_{\bar{\mathbf{b}}} = \left\{ \bar{\mathbf{V}}B(\bar{\mathbf{b}} + \bar{\boldsymbol{\alpha}}) \mid \forall \bar{\boldsymbol{\alpha}} \in [0, 1)^{D-1} \right\}, \quad (17)$$

where $\bar{\mathbf{b}} = [b_2, \dots, b_D]$ and $B \in \mathbb{R}_+^*$ is the polytope edge length along directions parallel with versors $\mathbf{v}_2, \dots, \mathbf{v}_D$. The set $\mathcal{P}_{\bar{\mathbf{b}}}$ is created via the last $D - 1$ vectors of the lattice basis $\mathbf{v}_2, \dots, \mathbf{v}_D$ where the basis coordinates lie in a set of rectangular polytopes $\mathcal{R}_{\bar{\mathbf{b}}}$ such that $\mathcal{P}_{\bar{\mathbf{b}}} = \{\bar{\mathbf{V}}\bar{\mathbf{x}} \mid \bar{\mathbf{x}} \in \mathcal{R}_{\bar{\mathbf{b}}}\}$, where

$$\mathcal{R}_{\bar{\mathbf{b}}} = \left\{ B(\bar{\mathbf{b}} + \bar{\boldsymbol{\alpha}}) \mid \bar{\boldsymbol{\alpha}} \in [0, 1)^{D-1} \right\} = \prod_{d=2}^D [b_d B, (b_d + 1) B]. \quad (18)$$

Note that $\mathbb{R}^{D-1} = \bigcup_{\bar{\mathbf{b}} \in \mathbb{Z}^{D-1}} \mathcal{P}_{\bar{\mathbf{b}}}$. Sets $\mathcal{P}_{\bar{\mathbf{b}}}$ thus can be used to split the domain of function f in disjoint *bands* of width B given by $\mathcal{B}_{\bar{\mathbf{b}}} = (\mathbb{R}\mathbf{v}_1) \times \mathcal{P}_{\bar{\mathbf{b}}}$ identified using the indices in $\bar{\mathbf{b}}$, such that $\mathbb{R}^D = \bigcup_{\bar{\mathbf{b}} \in \mathbb{Z}^{D-1}} \mathcal{B}_{\bar{\mathbf{b}}}$. By exploiting the smoothness of f

we can derive that, for a fixed $x_1 \in \mathbb{R}$, f has bounded variation within each band, and thus the folding can occur simultaneously on all coordinates x_2, \dots, x_D , which gives the folded signal a particular structure to be exploited in recovery. The definition of the new operator is given as follows.

Definition 2 (Multi-dimensional modulo-hysteresis). *The operator $\mathcal{M}_{\mathbf{H}}^D$ with threshold λ and hysteresis $h \in [0, 2\lambda/3)$, where $\mathbf{H} = [\lambda \ h]$, generates a function z for input $f \in \text{PW}_{\Omega}(\mathbb{R}^D)$ such that, for $[\mathbf{x}]_1 = x_1 \geq 0$*

$$z(\mathbf{V}\mathbf{x}) = f(\mathbf{V}\mathbf{x}) - \varepsilon_f(\mathbf{V}\mathbf{x}), \quad (19)$$

where ε_f denotes the modulo-hysteresis residual defined as

$$\varepsilon_f(\mathbf{V}\mathbf{x}) = h \left[M_{\bar{\mathbf{b}}} + \sum_{r=0}^{R_{\bar{\mathbf{b}}}^+} s_{\bar{\mathbf{b}},r} \mathbb{1}_{[\tau_{\bar{\mathbf{b}},r}, \infty)}(x_1) \right], \forall \bar{\mathbf{x}} = [x_2, \dots, x_D] \in \mathcal{R}_{\bar{\mathbf{b}}}, \quad (20)$$

where $\mathcal{R}_{\bar{\mathbf{b}}}$ satisfies (18), $\mathbf{x} = [x_1, \dots, x_D]$, $\bar{\mathbf{x}} = [x_2, \dots, x_D]$, and $M_{\bar{\mathbf{b}}} \in \mathbb{Z}$ satisfies

$$M_{\bar{\mathbf{b}}} = \left\lfloor \frac{\inf_{\bar{\mathbf{x}} \in \mathcal{R}_{\bar{\mathbf{b}}}} f_{\bar{\mathbf{x}}}(0) + \lambda}{h} \right\rfloor - 1, \quad (21)$$

and $\tau_{\bar{\mathbf{b}},r} \in \{0, \dots, R_{\bar{\mathbf{b}}}^+\}$, $s_{\bar{\mathbf{b}},r} \in \{-1, 0, 1\}$ are the folding times and signs in band $\mathcal{B}_{\bar{\mathbf{b}}}$, respectively, defined as

$$\tau_{\bar{\mathbf{b}},r+1} = \inf \left\{ x_1 > \tau_{\bar{\mathbf{b}},r} \mid \sup_{\bar{\mathbf{x}} \in \mathcal{R}_{\bar{\mathbf{b}}}} |f_{\bar{\mathbf{x}}}(x_1) - \varepsilon_{\bar{\mathbf{b}},r}(x_1)| = \lambda \right\}, \quad (22)$$

$$s_{\bar{\mathbf{b}},r+1} = \text{sign} [f_{B\bar{\mathbf{b}}}(\tau_{\bar{\mathbf{b}},r+1}) - \varepsilon_{\bar{\mathbf{b}},r}(\tau_{\bar{\mathbf{b}},r+1})], \quad (23)$$

$$\varepsilon_{\bar{\mathbf{b}},r+1}(x_1) = \varepsilon_{\bar{\mathbf{b}},r}(x_1) + h s_{\bar{\mathbf{b}},r+1} \mathbb{1}_{[\tau_{\bar{\mathbf{b}},r+1}, \infty)}(x_1), \quad (24)$$

where $r \in \{0, \dots, R_{\bar{\mathbf{b}}}^+ - 1\}$, $\varepsilon_{\bar{\mathbf{b}},r}$ is a recursive sequence of functions for computing the residual ε_f such that $\varepsilon_{\bar{\mathbf{b}},0}(x_1) = h M_{\bar{\mathbf{b}}}$, $\varepsilon_{\bar{\mathbf{b}},R_{\bar{\mathbf{b}}}^+}(x_1) = \varepsilon_f(\mathbf{V}\mathbf{x})$, $\bar{\mathbf{x}} \in \mathcal{R}_{\bar{\mathbf{b}}}$ and $\tau_{\bar{\mathbf{b}},0} = s_{\bar{\mathbf{b}},0} = 0$. Furthermore $R_{\bar{\mathbf{b}}}^+ \in \mathbb{Z}_+$ satisfies

$$\left\{ x_1 > \tau_{\bar{\mathbf{b}},R_{\bar{\mathbf{b}}}^+} \mid \sup_{\bar{\mathbf{x}} \in \mathcal{R}_{\bar{\mathbf{b}}}} |f_{\bar{\mathbf{x}}}(x_1) - \varepsilon_{\bar{\mathbf{b}},R_{\bar{\mathbf{b}}}^+}(x_1)| = \lambda \right\} = \emptyset. \quad (25)$$

Furthermore, for $x_1 < 0$ we have

$$\mathcal{M}_{\mathbf{H}}^D f(\mathbf{V}\mathbf{x}) = \mathcal{M}_{\mathbf{H}}^D [f^-](-x_1 \mathbf{v}_1 + x_2 \mathbf{v}_2 + \dots + x_D \mathbf{v}_D),$$

where $f^-(\mathbf{x}) = f_{\bar{\mathbf{x}}}(-x_1)$. Let $\tau_{\bar{\mathbf{b}},r}^-, s_{\bar{\mathbf{b}},r}^-, r \geq 1$ be the folding times and signs computed via (22), (23) for $\mathcal{M}_{\mathbf{H}}^D[f^-]$. Then we define $\tau_r \triangleq -\tau_{-r}^-, s_r \triangleq s_{-r}^-, r \in \mathbb{Z}, r < 0$.

We note that the operator in Definition 2 is backwards compatible with the one-dimensional operator in Definition 1. Specifically, if one chooses $\mathcal{R}_{\bar{\mathbf{b}}}$ to be a single point $\mathcal{R}_{\bar{\mathbf{b}}} = B\bar{\mathbf{b}} \in \mathbb{R}^{D-1}$ instead of a hypercube, then $\tau_{\bar{\mathbf{b}},r}$ and $s_{\bar{\mathbf{b}},r}$ in (22) are the same as τ_r in Definition 1. Furthermore, it was shown that, for $h = 0$, the one-dimensional modulo-hysteresis operator in Definition 1 is identical to an ideal modulo operator (4) [14].

3.4. Properties of the proposed operator

In the following we give a number of properties of the multi-dimensional modulo-hysteresis operator for a bandlimited input.

Proposition 2 (Folding time separation). *Assume that $\tau_{\bar{\mathbf{b}},r}$ are well-defined in (22) for $f \in \text{PW}_{\Omega}(\mathbb{R}^D)$ and $r \in \{1, \dots, R\}$ where $R \geq 1$ and $\tau_{\bar{\mathbf{b}},0} = 0$. Furthermore, assume that $\mathcal{D}f < \min\{h/2, 2\lambda - 3h\}$, where*

$$\mathcal{D}f \triangleq \sup_{\substack{\bar{\mathbf{b}} \in \mathbb{Z}^{D-1} \\ x_1 \in \mathbb{R}}} \left[\sup_{\bar{\mathbf{x}} \in \mathcal{R}_{\bar{\mathbf{b}}}} f_{\bar{\mathbf{x}}}(x_1) - \inf_{\bar{\mathbf{x}} \in \mathcal{R}_{\bar{\mathbf{b}}}} f_{\bar{\mathbf{x}}}(x_1) \right]. \quad (26)$$

Then

$$\tau_{\bar{\mathbf{b}},r+1} - \tau_{\bar{\mathbf{b}},r} \geq \frac{h}{\Omega_1 \|f\|_{\infty}}, \quad \forall \bar{\mathbf{b}} \in \mathbb{Z}^{D-1}. \quad (27)$$

Proof. The proof is in Section 7.1. □

Proposition 3 (Well-defined operator). *For input $f \in \text{PW}_{\Omega}(\mathbb{R}^D)$ operator $\mathcal{M}_{\mathbf{H}}^D$ in Definition 1 is well-defined if $\mathcal{D}f < \min\{h/2, 2\lambda - 3h\}$, where $\mathcal{D}f$ satisfies (26).*

Proof. The proof is in Section 7.1. □

Proposition 4 (Modulo output dynamic range). *Let $\mathcal{M}_{\mathbf{H}}^D$ be the multi-dimensional modulo-hysteresis operator in Definition 2 and $f \in \text{PW}_{\Omega}(\mathbb{R}^D)$ such that $\mathcal{D}f$ (26) satisfies $\mathcal{D}f < \min\{h/2, 2\lambda - 3h\}$. Then $\mathcal{M}_{\mathbf{H}}^D f(\mathbf{x}) \in [-\lambda, \lambda], \forall \mathbf{x} \in \mathbb{R}^D$.*

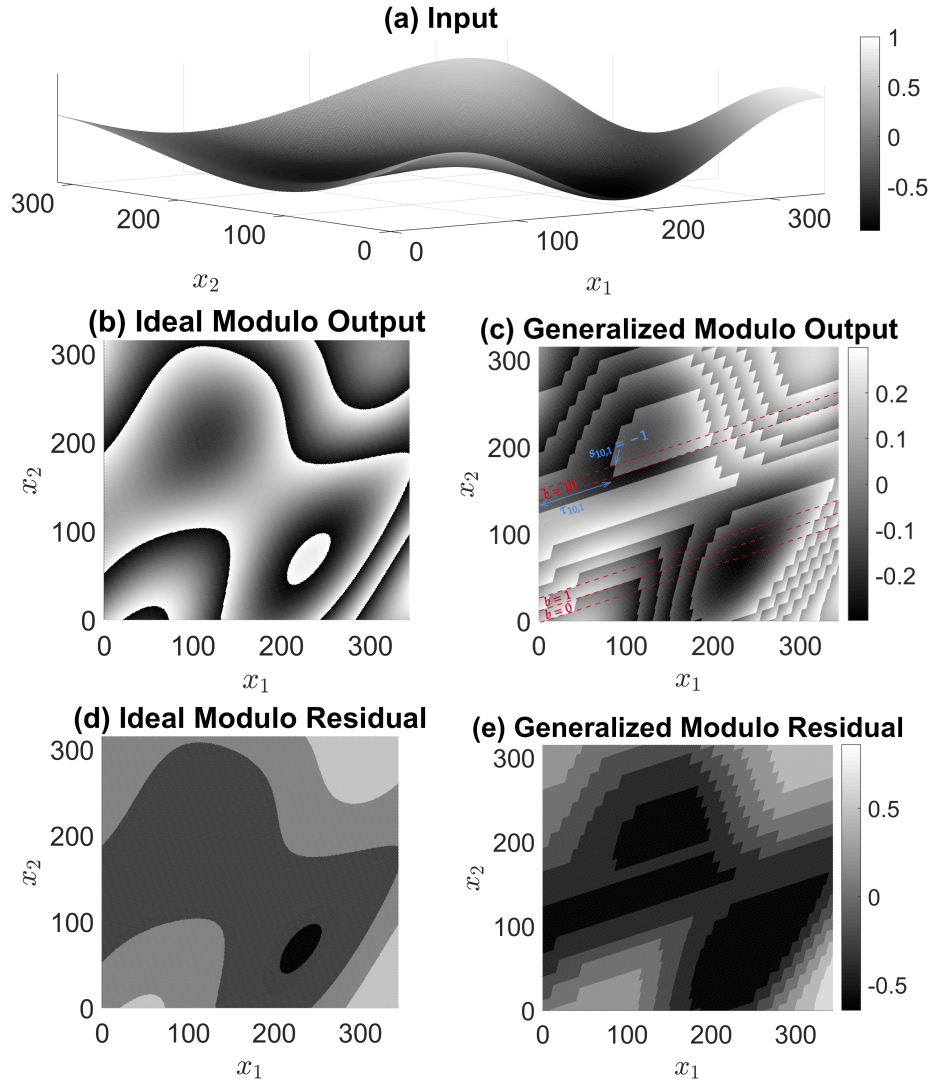


Figure 2: A random two-dimensional bandlimited input $f(x_1, x_2)$ was generated (a). The ideal modulo output $\mathcal{M}_\lambda f$ is in (b) and the generalized modulo output $\mathcal{M}_\mathbf{H}^D f$ in (c). The corresponding residual functions are depicted in (d) for ideal modulo and in (e) for generalized modulo. For $\mathcal{M}_\mathbf{H}^D$, the lattice $\mathbf{\Lambda}$ consists of vectors $\mathbf{v}_1 = [0.97, 0.25]^\top$, $\mathbf{v}_2 = [0.32, 0.95]^\top$. The folding curves of the ideal modulo – the contours in (b) & (d) – are unknown *a priori*. In the case of the modulo-hysteresis, folding occurs along straight lines with directions dictated by the lattice $\mathbf{\Lambda}$ which is known *a priori*. This property will be exploited in recovery.

Proof. The proof is in Section 7.1. \square

Proposition 4 shows that operator $\mathcal{M}_{\mathbf{H}}^D$ has a similar effect as the one-dimensional modulo nonlinearity, in that it keeps a signal within a fixed dynamic range $[-\lambda, \lambda]$.

Corollary 1 (Bound for intra-band variation). *The quantity $\mathcal{D}f$ defined in Proposition 2 can be bounded as*

$$\mathcal{D}f \leq \|f\|_{\infty} \cdot B\sqrt{D} \cdot \|\Omega\|_2. \quad (28)$$

Proof. The proof is in Section 7.1. \square

In Fig. 2 the variation of $M_{\bar{\mathbf{b}}}$, which can be seen as folds along coordinates x_2, \dots, x_D for $x_1 = 0$, is *gradual*, meaning that $M_{\bar{\mathbf{b}}}$ changes by 1 between neighboring bands. Formally, we define by $\text{Neighbors}(\bar{\mathbf{b}})$ the set comprising all neighboring bands of band $\bar{\mathbf{b}}$ below.

Definition 3 (Neighboring bands). *The set $\text{Neighbors}(\bar{\mathbf{b}})$ of vectors neighboring $\bar{\mathbf{b}} \in \mathbb{Z}^{D-1}$ is defined as the set of all $\bar{\mathbf{b}}^* \in \mathbb{Z}^{D-1}$ for which $\exists d^* \in \{2, \dots, D\}$ such that $|\bar{\mathbf{b}}^*_{d^*} - \bar{\mathbf{b}}_{d^*}| = 1$ and $\bar{\mathbf{b}}_d = \bar{\mathbf{b}}^*_d, \forall d \in \{2, \dots, D\} \setminus d^*$.*

In the following, we provide conditions for which $M_{\bar{\mathbf{b}}^*} - M_{\bar{\mathbf{b}}} \in \{-1, 0, 1\}$ where $\bar{\mathbf{b}}^* \in \text{Neighbors}(\bar{\mathbf{b}})$.

Proposition 5 (Variation of $M_{\bar{\mathbf{b}}}$). *For $\forall \bar{\mathbf{b}} \in \mathbb{Z}^{D-1}$, let $\bar{\mathbf{b}}^* \in \text{Neighbors}(\bar{\mathbf{b}})$. Let $M_{\bar{\mathbf{b}}^*}$ and $M_{\bar{\mathbf{b}}}$ be the modulo-hysteresis constants for an input $f \in \text{PW}_{\Omega}(\mathbb{R}^D)$ satisfying the following condition as per Definition 2*

$$\|f\|_{\infty} B\sqrt{D} \cdot \sqrt{\sum_{d=1}^D \Omega_d^2} < \min \left\{ \frac{h}{2}, 2\lambda - 3h \right\}. \quad (29)$$

Then $M_{\bar{\mathbf{b}}^} - M_{\bar{\mathbf{b}}} \in \{-1, 0, 1\}$.*

Proof. We first note that sets $\mathcal{R}_{\bar{\mathbf{b}}}$ and $\mathcal{R}_{\bar{\mathbf{b}}^*}$ are neighboring polytopes which, via their definition, satisfy $\text{cl}(\mathcal{R}_{\bar{\mathbf{b}}}) \cap \text{cl}(\mathcal{R}_{\bar{\mathbf{b}}^*}) \neq \emptyset$. Using this in conjunction with the properties of supremum and infimum, we get

$$\sup_{\bar{\mathbf{x}} \in \mathcal{R}_{\bar{\mathbf{b}}}} f_{\bar{\mathbf{x}}}(0) = \max_{\bar{\mathbf{x}} \in \text{cl}(\mathcal{R}_{\bar{\mathbf{b}}})} f_{\bar{\mathbf{x}}}(0) \geq \min_{\bar{\mathbf{x}} \in \text{cl}(\mathcal{R}_{\bar{\mathbf{b}}^*})} f_{\bar{\mathbf{x}}}(0) = \inf_{\bar{\mathbf{x}} \in \mathcal{R}_{\bar{\mathbf{b}}^*}} f_{\bar{\mathbf{x}}}(0). \quad (30)$$

Condition (29) implies $\mathcal{D}f < h/2$ due to Corollary 1. Therefore,

$$\sup_{\bar{\mathbf{x}} \in \mathcal{R}_{\bar{\mathbf{b}}}} f_{\bar{\mathbf{x}}}(0) - \inf_{\bar{\mathbf{x}} \in \mathcal{R}_{\bar{\mathbf{b}}}} f_{\bar{\mathbf{x}}}(0) < h/2. \quad (31)$$

Using (30) and (31)

$$\inf_{\bar{\mathbf{x}} \in \mathcal{R}_{\bar{\mathbf{b}}^*}} f_{\bar{\mathbf{x}}}(0) - \inf_{\bar{\mathbf{x}} \in \mathcal{R}_{\bar{\mathbf{b}}}} f_{\bar{\mathbf{x}}}(0) < h/2. \quad (32)$$

Given that, by definition, $M_{\bar{\mathbf{b}}^*} = \left\lfloor \frac{\inf_{\bar{\mathbf{x}} \in \mathcal{R}_{\bar{\mathbf{b}}^*}} f_{\bar{\mathbf{x}}}(0) + \lambda}{h} \right\rfloor - 1$, it can be shown by direct derivation that $M_{\bar{\mathbf{b}}^*} \leq M_{\bar{\mathbf{b}}} + 1$. Furthermore, by swapping $\bar{\mathbf{b}}$ and $\bar{\mathbf{b}}^*$ in the derivation above we get

$$M_{\bar{\mathbf{b}}} \in \{M_{\bar{\mathbf{b}}^*} - 1, M_{\bar{\mathbf{b}}^*}, M_{\bar{\mathbf{b}}^*} + 1\}. \quad (33)$$

□

Therefore, using Definition 2, for $x_1 = 0$, in neighboring bands $\bar{\mathbf{b}}$ and $\bar{\mathbf{b}}^*$ the residual ε_f is either the same, or differs by h . This is similar to the behavior of the residual around a folding time $\tau_{\bar{\mathbf{b}},r}$ along dimension x_1 .

3.5. Problem formulation

The measurements $y[\mathbf{k}]$ are assumed to be samples on a multi-dimensional lattice $\Lambda = \{\mathbf{V}\mathbf{T}\mathbf{k} | \mathbf{k} \in \mathbb{Z}^D\}$, such that

$$y[\mathbf{k}] = \mathcal{M}_{\mathbf{H}}^D f(\mathbf{V}\mathbf{T}\mathbf{k}) + \eta[\mathbf{k}] = \gamma[\mathbf{k}] - \varepsilon_\gamma[\mathbf{k}] + \eta[\mathbf{k}], \quad (34)$$

where $\gamma[\mathbf{k}] = f(\mathbf{V}\mathbf{T}\mathbf{k})$, $\varepsilon_\gamma[\mathbf{k}] = \varepsilon_f(\mathbf{V}\mathbf{T}\mathbf{k})$ and $\eta[\mathbf{k}] \sim \mathcal{N}(0, \sigma^2)$. The known variables are the input bandwidth Ω , number of dimensions D , the lattice Λ , modulo-hysteresis parameters B, λ, h and output samples $y[\mathbf{k}]$. The proposed reconstruction problem is to compute the input lattice samples $\tilde{\gamma}[\mathbf{k}]$ defined as

$$\tilde{\gamma}[\mathbf{k}] = \gamma[\mathbf{k}] + \eta[\mathbf{k}] + Mh, \quad (35)$$

where $M \in \mathbb{Z}$ is an unknown integer. The input $\gamma[\mathbf{k}]$ can only be reconstructed up to an integer multiple of h given that $\mathcal{M}_{\mathbf{H}}^D f(\mathbf{x}) = \mathcal{M}_{\mathbf{H}}^D [f + Mh](\mathbf{x}), \forall M \in \mathbb{Z}$ (19,20).

4. Detecting modulo-hysteresis discontinuities

We define $N_d^B = \frac{B}{T_d}$. For simplicity, we assume that $N_d^B \in \mathbb{Z}, N_d^B \geq 1, \forall d \in \{2, \dots, D\}$, i.e., for a polytope $\mathcal{P}_{\bar{\mathbf{b}}}$ we have an integer number of sampling periods T_d along each of its edges of length B and direction \mathbf{v}_d . The recovery is achieved in several steps

1. Compute $M_{\bar{\mathbf{b}}}$, the folding times $\tau_{\bar{\mathbf{b}},r}$ and signs $s_{\bar{\mathbf{b}},r}$ in each band $\mathcal{B}_{\bar{\mathbf{b}}}$.
2. Compute residual $\varepsilon_f(\mathbf{V}\mathbf{x})$ (20).
3. Compute the samples $\tilde{\gamma}[\mathbf{k}]$.

For step 1, we define a filter ψ and compute $\langle y, \psi \rangle$. For detecting the folding times and signs, we choose $\psi = \psi_{\bar{\mathbf{b}},m}$, which is centered in sample m along dimension x_1 in band $\bar{\mathbf{b}}$ as

$$\psi_{\bar{\mathbf{b}},m}[\mathbf{k}] = \begin{cases} \Delta^N [k_1 - m] \cdot \frac{1}{N^B}, & \bar{\mathbf{T}}\bar{\mathbf{k}} \in \mathcal{R}_{\bar{\mathbf{b}}}, \\ 0, & \bar{\mathbf{T}}\bar{\mathbf{k}} \notin \mathcal{R}_{\bar{\mathbf{b}}}, \end{cases} \quad (36)$$

where $\bar{\mathbf{k}} \in \mathbb{Z}^{D-1}$ and $N^B = \prod_{d=2}^D N_d^B$ is the number of samples in each band $\bar{\mathbf{b}}$ for k_1 fixed. For fixed $\bar{\mathbf{k}} \in \mathbb{Z}^{D-1}$, $\psi_{\bar{\mathbf{b}},m}[\mathbf{k}]$ is a finite difference filter along dimension k_1 .

For detecting the $M_{\bar{\mathbf{b}}}$, we need a filter detecting the change in $M_{\bar{\mathbf{b}}}$ for two bands $\bar{\mathbf{b}}, \bar{\mathbf{b}}^*$, such that $\bar{\mathbf{b}}^* \in \text{Neighbors}(\bar{\mathbf{b}})$ and $[\bar{\mathbf{b}}^*]_{d^*} = [\bar{\mathbf{b}}]_{d^*} + 1$. We define $\psi = \psi_{\bar{\mathbf{b}},\bar{\mathbf{b}}^*}[\mathbf{k}]$ as

$$\psi_{\bar{\mathbf{b}},\bar{\mathbf{b}}^*}[\mathbf{k}] = \begin{cases} \Delta^N [k_{d^*} - k_{\bar{\mathbf{b}}}] \cdot \frac{1}{N^{B^*}}, & \bar{\mathbf{T}}\bar{\mathbf{k}} \in \mathcal{R}_{\bar{\mathbf{b}}} \cup \mathcal{R}_{\bar{\mathbf{b}}^*}, k_1 = 0, \\ 0, & \text{otherwise,} \end{cases} \quad (37)$$

where $k_{\bar{\mathbf{b}}} = N_{d^*}^B \cdot [\bar{\mathbf{b}}]_{d^*} - 1$ and $N^{B^*} = \prod_{d=2, d \neq d^*}^D N_d^B$ is the number of samples in each band $\bar{\mathbf{b}}$ for k_1, k_{d^*} fixed. Therefore, similar to $\psi_{\bar{\mathbf{b}},m}$, filter $\psi_{\bar{\mathbf{b}},\bar{\mathbf{b}}^*}$ is a finite difference filter along dimension x_{d^*} which is perpendicular to the hyperplane separating bands $\bar{\mathbf{b}}$ and $\bar{\mathbf{b}}^*$. Furthermore, $\psi_{\bar{\mathbf{b}},\bar{\mathbf{b}}^*}$ is constant within each band $\bar{\mathbf{b}}$ and $\bar{\mathbf{b}}^*$. This means that the finite difference filter is repeated N^{B^*} times across dimensions $d \in \{2, \dots, D\} \setminus d^*$, which has a noise averaging effect.

4.1. Detecting folding times and signs

To detect $\tau_{\bar{\mathbf{b}},r}$ and $s_{\bar{\mathbf{b}},r}$, we use filter $\psi_{\bar{\mathbf{b}},m}$ to compute sequence $y_{\bar{\mathbf{b}},m}$

$$y_{\bar{\mathbf{b}},m} = \langle y, \psi_{\bar{\mathbf{b}},m} \rangle = \underbrace{\langle \gamma, \psi_{\bar{\mathbf{b}},m} \rangle}_{\text{Input}} - \underbrace{\langle \varepsilon_\gamma, \psi_{\bar{\mathbf{b}},m} \rangle}_{\text{Residual}} + \underbrace{\langle \eta, \psi_{\bar{\mathbf{b}},m} \rangle}_{\text{Noise}}. \quad (38)$$

In (38) the filtered samples $y_{\bar{\mathbf{b}},m}$ are composed of three terms: the *input term* $\langle \gamma, \psi_{\bar{\mathbf{b}},m} \rangle$, the *residual term* $\langle \varepsilon_\gamma, \psi_{\bar{\mathbf{b}},m} \rangle$ and the *noise term* $\langle \eta, \psi_{\bar{\mathbf{b}},m} \rangle$. Given that all three are unknown, the general recovery strategy is to separate them via thresholding; as will be shown later, thresholding samples $y_{\bar{\mathbf{b}},m}$ allows to compute the folding times and signs. While this will be derived rigorously later in propositions 6 and 7, here we give a brief intuitive explanation of the recovery method, by explaining the effect that filter $\psi_{\bar{\mathbf{b}},m}$ has on all 3 terms in the right-hand-side of (38). A similar analysis applies to filter $\psi_{\bar{\mathbf{b}},\bar{\mathbf{b}}^*}$ which will be described in Section 4.2.

As noted before, $\psi_{\bar{\mathbf{b}},m}$ is a finite difference filter along dimension x_1 . It was shown for the one-dimensional case that this causes $\gamma[\mathbf{k}]$ to vanish for large N . Furthermore, it generates peaks at the folding times in residual ε_γ and also amplifies the noise η [12, 14]. This latter effect is undesirable for recovery. To decrease the effect of the noise the finite difference filter was convolved with a spline in the one-dimensional case, but this also makes the detection of ε_γ more difficult [34]. Here we can address noise filtering without affecting the folding time detection by exploiting the multi-dimensional structure of $\mathcal{M}_{\mathbf{H}}^D$.

For fixed $k_1 \in \mathbb{Z}$, the filter $\psi_{\bar{\mathbf{b}},m}[\mathbf{k}]$ is constant along dimensions k_2, \dots, k_D as long as $\bar{\mathbf{V}}^T \bar{\mathbf{T}} \bar{\mathbf{k}} \in \mathcal{R}_{\bar{\mathbf{b}}}$ and thus the inner product has an averaging effect. However, we know that the modulo residual corresponding to $\mathcal{M}_{\mathbf{H}}^D f(\mathbf{V}\mathbf{x})$, $\bar{\mathbf{x}} \in \mathcal{R}_{\bar{\mathbf{b}}}$ is also constant within $\mathcal{R}_{\bar{\mathbf{b}}}$ by definition, and therefore the averaging effect does not affect the residual edges, which are along dimension k_1 . Moreover, given that f is smooth and changes slowly within a band $\mathcal{B}_{\bar{\mathbf{b}}}$, the filter averaging along dimensions $\bar{\mathbf{k}}$ has very little effect on γ . Therefore, along dimensions $\bar{\mathbf{k}}$, the filter acts mainly on the noise sequence $\eta[\bar{\mathbf{k}}]$ by narrowing its p.d.f. around the origin such that its effect gradually vanishes.

As in the one-dimensional case, the modulo output z is smooth in-between the folds, and has discontinuities at the folding times. The filter $\psi_{\bar{\mathbf{b}},m}$ responds with pulses

of non-zero support to the input discontinuities. To account for this, we define by \mathbb{S}_N the support of the filtered residual such that (see [14] for details)

$$\mathbb{S}_N = \text{supp} [\langle \varepsilon_\gamma, \psi_{\bar{\mathbf{b}}, m} \rangle] = \bigcup_{r \in \mathbb{Z}^*} \left\{ \left[\frac{\tau_{\bar{\mathbf{b}}, r}}{T_1} \right] - N, \dots, \left[\frac{\tau_{\bar{\mathbf{b}}, r}}{T_1} \right] \right\}.$$

The following theorem shows how \mathbb{S}_N can be recovered by thresholding sequence $\langle y, \psi_{\bar{\mathbf{b}}, m} \rangle$, which is an important step in computing folding times $\tau_{\bar{\mathbf{b}}, r}$.

Proposition 6 (Detection of folding times). *Let $f \in \text{PW}_\Omega(\mathbb{R}^D)$ and let $z(\mathbf{x}) = \mathcal{M}_{\mathbf{H}}^D f(\mathbf{x})$ be the output of a multi-dimensional modulo-hysteresis model with parameters λ, h, B . Furthermore, let $y[\mathbf{k}] = z(\mathbf{V}\mathbf{T}\mathbf{k}) + \eta[\mathbf{k}]$ be the samples of the modulo output computed on lattice $\mathbf{\Lambda}$ corrupted by a noise sequence $\eta[\mathbf{k}] \sim \mathcal{N}(0, \sigma^2)$. Furthermore, assume that $T_d < B, \forall d \in \{2, \dots, D\}$ and that*

$$\|f\|_\infty B \sqrt{D} \cdot \sqrt{\sum_{d=1}^D \Omega_d^2} < \min \left\{ \frac{h}{2}, 2\lambda - 3h \right\}, \quad (39)$$

$$(T_1 \Omega_1 e)^N \|f\|_\infty < h/2.$$

If $|\langle y, \psi_{\bar{\mathbf{b}}, m} \rangle| \geq h/2$ then $m \in \mathbb{S}_N$ with probability $p > 1 - p_{\text{err}}$ where

$$p_{\text{err}} \leq e^{-C^2}, \quad \text{where } C = \frac{h/2 - (T_1 \Omega_1 e)^N \|f\|_\infty}{\sigma \sqrt{2^{N+1}}} \prod_{d=2}^D \sqrt{\frac{B}{T_d}}. \quad (40)$$

Proof. The proof is in Section 7.2. □

Due to Proposition 6, for $\forall \sigma, \lambda, h, \mathbf{\Omega} \in \mathbb{R}_+^D$ satisfying (39) and a fixed $m \in \mathbb{Z}$, one can choose $T_1, \dots, T_D > 0$ such that the truth value of $m \in \mathbb{S}_N$ is evaluated correctly with an arbitrarily large probability. We note that p_{err} measures the probability when a recovery error is possible, but not guaranteed, therefore the error probability is smaller in a real scenario. A small error in Proposition 6 means a large C , which can be achieved by decreasing the sampling periods T_1, \dots, T_d or increasing B, h or number of dimensions D .

The residual ε_γ , used for reconstructing γ , requires detecting constants $M_{\bar{\mathbf{b}}}$ in addition to the folding times $\tau_{\bar{\mathbf{b}}, r}$ and signs $s_{\bar{\mathbf{b}}, r}$, as will be explained in the next subsection.

4.2. Detecting constants $M_{\bar{\mathbf{b}}}$

Given that we can only recover γ up to an integer multiple of h (35), we define $\widetilde{M}_{\bar{\mathbf{b}}} \triangleq M_{\bar{\mathbf{b}}} - M_{\bar{\mathbf{0}}}$, where $\bar{\mathbf{0}}$ is the null vector of \mathbb{Z}^{D-1} , and recover $\widetilde{M}_{\bar{\mathbf{b}}}$. Just as the folding times, different values of $M_{\bar{\mathbf{b}}}$ for adjacent bands cause discontinuities. However, unlike the detection of the folding times, here we have additional information. Specifically, we know that the discontinuities may only be located at the neighboring sides of polytopes $\mathcal{P}_{\bar{\mathbf{b}}}$. We use the filter $\psi_{\bar{\mathbf{b}}, \bar{\mathbf{b}}^*}$ (37) to detect the discontinuities in a similar fashion to detecting the folding times via $\psi_{\bar{\mathbf{b}}, m}$. This time, however, the finite differences Δ^N computed via $\psi_{\bar{\mathbf{b}}, \bar{\mathbf{b}}^*}$ evaluate variations across dimensions x_2, \dots, x_D .

Proposition 7 (Detection of constants $M_{\bar{\mathbf{b}}}$). *Let $y[\mathbf{k}] = z(\mathbf{V}\mathbf{T}\mathbf{k}) + \eta[\mathbf{k}]$, where $\eta[\mathbf{k}] \sim \mathcal{N}(0, \sigma^2)$ and $z(\mathbf{x})$ is the output of a modulo-hysteresis operator $z(\mathbf{x}) = \mathcal{M}_{\mathbf{H}}^D f(\mathbf{x})$ with parameters λ, h and $f \in \text{PW}_{\Omega}(\mathbb{R}^D)$ satisfying*

$$\|f\|_{\infty} B \sqrt{D} \cdot \sqrt{\sum_{d=1}^D \Omega_d^2} < \min\{h/2, 2\lambda - 3h\}, \quad (41)$$

Furthermore, let $\bar{\mathbf{b}} \in \mathbb{Z}^{D-1}$, $\bar{\mathbf{b}}^* \in \text{Neighbors}(\bar{\mathbf{b}})$ and $d^* \in \{2, \dots, D\}$ such that $[\bar{\mathbf{b}}^*]_{d^*} = [\bar{\mathbf{b}}]_{d^*} + 1$. Assume that

$$(T_{d^*} \Omega_{d^*} e)^N \|f\|_{\infty} < h/2, \quad (42)$$

$$(N+1) T_{d^*} < B. \quad (43)$$

Then the following is true with probability $p > 1 - p_{\text{err}}$

$$\begin{cases} M_{\bar{\mathbf{b}}^*} = M_{\bar{\mathbf{b}}} + \text{sign}(\langle y, \psi_{\bar{\mathbf{b}}, \bar{\mathbf{b}}^*} \rangle) & \text{if } |\langle y, \psi_{\bar{\mathbf{b}}, \bar{\mathbf{b}}^*} \rangle| \geq h/2, \\ M_{\bar{\mathbf{b}}^*} = M_{\bar{\mathbf{b}}} & \text{otherwise.} \end{cases} \quad (44)$$

where

$$p_{\text{err}} \leq e^{-\kappa^2}, \quad \text{where } \kappa = \frac{h/2 - (T_{d^*} \Omega_{d^*} e)^N \|f\|_{\infty}}{\sigma \sqrt{2^{N+1}}} \prod_{d=2, d \neq d^*}^D \sqrt{\frac{B}{T_d}}. \quad (45)$$

Proof. The proof is in Section 7.2. □

5. Input reconstruction

5.1. Recovery with the proposed operator

We begin with the noiseless input recovery scenario $\sigma = 0$ where, via Proposition 6, the set \mathbb{S}_N is perfectly identified with probability 1. Furthermore, a constant $\widetilde{M}_{\bar{\mathbf{b}}} = M_{\bar{\mathbf{b}}} - M_{\mathbf{0}}$ can be perfectly recovered from $\widetilde{M}_{\bar{\mathbf{b}}^*}$ where $\bar{\mathbf{b}}^* \in \text{Neighbors}(\bar{\mathbf{b}})$ according to Proposition 7. The following theorem proves the input recovery conditions in the case $\sigma = 0$.

Theorem 2 (Noiseless input reconstruction). *Let $f \in \text{PW}_{\Omega}(\mathbb{R}^D)$ and let $z(\mathbf{x}) = \mathcal{M}_{\mathbf{H}}^D f(\mathbf{x})$ be the output of a multi-dimensional modulo-hysteresis model with parameters λ, h, B . Furthermore, let $y[\mathbf{k}] = z(\mathbf{V}\mathbf{T}\mathbf{k})$ be the samples of the modulo output computed on lattice $\mathbf{\Lambda}$. Furthermore, for $N \in \mathbb{Z}, N \geq 1$, assume that*

$$\|f\|_{\infty} B \sqrt{D} \cdot \|\Omega\|_2 < \min\{h/2, 2\lambda - 3h\}, \quad (46)$$

$$(T_d \Omega_d e)^N \|f\|_{\infty} < h/2, \quad \forall d \in \{1, \dots, D\}, \quad (47)$$

$$(N+1)T_1 < \frac{h}{\Omega_1 \|f\|_{\infty}}, \quad (48)$$

$$(N+1)T_d < B, \quad \forall d \in \{2, \dots, D\}. \quad (49)$$

Then samples $\tilde{\gamma}[\mathbf{k}] = \gamma[\mathbf{k}] - hM_{\mathbf{0}}$ can be perfectly reconstructed from $y[\mathbf{k}]$.

Proof. The proof is in Section 7.2. □

The interpretation of the sufficient conditions in Theorem 2 is as follows. The modulo-hysteresis is well-defined due to a bounded intra-band variation guaranteed by (46). Condition (47) bounds the N -th order difference of the input along all of the dimensions, ensuring that the filter has enough shrinking effect on the input. Finally, (48) and (49) guarantee enough samples in between the folds (48) and within each band (49) so that the supports of the filters detecting consecutive discontinuities don't overlap.

In the general case where $\sigma > 0$ the following result holds true.

Theorem 3 (Noisy input reconstruction). *Let $f \in \text{PW}_{\Omega}(\mathbb{R}^D)$ and $z(\mathbf{x}) = \mathcal{M}_{\mathbf{H}}^D f(\mathbf{x})$. Assume that $y[\mathbf{k}] = z(\mathbf{V}\mathbf{T}\mathbf{k}) + \eta[\mathbf{k}]$ are known for $k_d \in \{1, \dots, K_{\max}^d\}$ where*

$\eta[\mathbf{k}] \sim \mathcal{N}(0, \sigma^2)$, such that $B_{\max}^d \triangleq \frac{K_{\max}^d}{N_{\max}^d} \in \mathbb{Z}$ for $d \in \{2, \dots, D\}$. Then, if (46-49) are true, then the input samples $\tilde{\gamma}[\mathbf{k}]$ can be recovered from $y[\mathbf{k}]$ with a probability $p > p_{\text{acc}}$ such that

$$p_{\text{acc}} \geq \left(1 - e^{-C^2}\right)^{K_{\max}^1 \cdot \prod_{d=2}^D B_{\max}^d} \cdot \left(1 - e^{-\kappa_{\min}^2}\right)^{\prod_{d=2}^D B_{\max}^d},$$

where

$$C = \frac{h/2 - (T_1 \Omega_1 e)^N \|f\|_{\infty}}{\sigma \sqrt{2^{N+1}}} \prod_{d=2}^D \sqrt{\frac{B}{T_d}},$$

$$\kappa_{\min} = \frac{h/2 - [(\max_d T_d \Omega_d) \cdot e]^N \|f\|_{\infty}}{\sigma \sqrt{2^{N+1}}} \sqrt{\frac{B^{D-2}}{T_{\max}^{D-2}}},$$

where $T_{\max} = \max_{d \in \{2, \dots, D\}} T_d$.

Proof. Theorem 2 assumes that Proposition 6 and 7 hold with $p_{\text{err}} = 0$ for all filters $\psi_{\bar{\mathbf{b}}, m}$ and $\psi_{\bar{\mathbf{b}}, \bar{\mathbf{b}}^*}$. To calculate the overall error probability when this assumption is not true, we count the filters above, when used in reconstruction, as follows. There are a total of $\prod_{d=2}^D B_{\max}^d$ bands, and K_{\max}^1 samples along dimension x_1 . Then the probability that Proposition 6 holds for all filters $\psi_{\bar{\mathbf{b}}, m}$ is $\left(1 - e^{-C^2}\right)^{K_{\max}^1 \cdot \prod_{d=2}^D B_{\max}^d}$.

Next, in the case of Proposition 7, we bound the error probability as follows

$$p_{\text{err}} \leq e^{-\kappa^2} \leq e^{-\kappa_{\min}^2}, \quad \kappa_{\min} = \frac{h/2 - [(\max_{d \in \{2, \dots, D\}} T_d \Omega_d) e]^N \|f\|_{\infty}}{\sigma \sqrt{2^{N+1}}} \cdot \sqrt{\frac{B^{D-2}}{T_{\max}^{D-2}}}. \quad (50)$$

We note that we do not use all filters $\psi_{\bar{\mathbf{b}}, \bar{\mathbf{b}}^*}$. Given that we use a set of samples that is contiguous along all dimensions, any band $\bar{\mathbf{b}}$ containing samples has at least one neighboring band $\bar{\mathbf{b}}^* \in \text{Neighbors}(\bar{\mathbf{b}})$ that contains samples. Then, each constant $\tilde{M}_{\bar{\mathbf{b}}} = M_{\bar{\mathbf{b}}} - M_{\bar{\mathbf{0}}}$ can be computed using a single evaluation of $\psi_{\bar{\mathbf{b}}, \bar{\mathbf{b}}^*}$, which, in total, is evaluated $\prod_{d=2}^D B_{\max}^d - 1$ times, and the theorem follows. \square

5.2. Comparison to ideal modulo recovery with Gaussian noise measurements

The USF was not analysed in the presence of Gaussian noise, but rather on bounded noise [12, 28]. However, USF can still be applied for recovery in the context of Gaussian noise, and the reconstruction would still be accurate in the instances when the noise sample with maximum amplitude satisfies the USF conditions. The modulo

operator with Gaussian noise was considered before, but the main objective was de-noising, rather than input reconstruction [32, 31]. In order to assess the advantage of the new $\mathcal{M}_{\mathbf{H}}^D$ operator, we provide some insight on reconstruction via USF for multi-dimensional inputs. Specifically, we note that, for an input $f \in \text{PW}_{\Omega}(\mathbb{R}^D)$ and a lattice Λ , the ideal modulo output is decomposed as (see also Section 2.1)

$$y[\mathbf{k}] = \gamma[\mathbf{k}] - \varepsilon_{\gamma}[\mathbf{k}] + \eta[\mathbf{k}].$$

The recovery method from [28] involves a *line-by-line* approach, meaning that the recovery is performed along dimension k_1 , $\forall \bar{\mathbf{k}} = [k_2, \dots, k_D]$. By defining $y_{\bar{\mathbf{k}}}[k_1] = y[\mathbf{k}]$, $\gamma_{\bar{\mathbf{k}}}[k_1] = \gamma[\mathbf{k}]$, $\varepsilon_{\gamma, \bar{\mathbf{k}}}[k_1] = \varepsilon_{\gamma}[\mathbf{k}]$, and $\eta_{\bar{\mathbf{k}}}[k_1] = \eta[\mathbf{k}]$, the recovery is performed by computing

$$\begin{aligned} \langle y_{\bar{\mathbf{k}}}, \Delta^N[\cdot - m] \rangle &= \langle \gamma_{\bar{\mathbf{k}}}, \Delta^N[\cdot - m] \rangle - \langle \varepsilon_{\gamma, \bar{\mathbf{k}}}, \Delta^N[\cdot - m] \rangle \\ &+ \langle \eta_{\bar{\mathbf{k}}}, \Delta^N[\cdot - m] \rangle. \end{aligned} \quad (51)$$

We remark that the processing in (51) is equivalent to applying filter $\psi_{\bar{\mathbf{b}}, m}$ (36) in the case of the multidimensional modulo-hysteresis operator when there is only one sample per band in all dimensions, i.e., $N_2^B = N_3^B = \dots = N_d^B = N^B = 1$. Even though the noise here is not bounded, we can derive the condition when the USF would work for a specific noise instance, which is [12]

$$|\langle \gamma_{\bar{\mathbf{k}}}, \Delta^N[\cdot - m] \rangle + \langle \eta_{\bar{\mathbf{k}}}, \Delta^N[\cdot - m] \rangle| \leq (T_1 \Omega_1 e)^N \|f\|_{\infty} + |\langle \eta_{\bar{\mathbf{k}}}, \Delta^N[\cdot - m] \rangle| < \lambda.$$

for all $m \in \mathbb{Z}$. Thus, recovery is only guaranteed if the noise instance is bounded by

$$|\langle \eta_{\bar{\mathbf{k}}}, \Delta^N[\cdot - m] \rangle| < \lambda - (T_1 \Omega_1 e)^N \|f\|_{\infty}. \quad (52)$$

In a similar fashion to the derivation of (98) it can be shown that $\langle \eta_{\bar{\mathbf{k}}}, \Delta^N[\cdot - m] \rangle \sim \mathcal{N}(0, \sigma^2 \cdot 2^N)$. We remark that the standard deviation of $\langle \eta_{\bar{\mathbf{k}}}, \Delta^N[\cdot - m] \rangle$ is always at least $\sigma\sqrt{2}$. Therefore, depending on the values of T_1 , Ω_1 and λ , the probability that (52) holds may be very low. Conversely, in the recovery with the proposed operator $\mathcal{M}_{\mathbf{H}}^D$, $\langle \eta_{\bar{\mathbf{k}}}, \psi_{\bar{\mathbf{b}}, m} \rangle$ satisfies $\langle \eta_{\bar{\mathbf{k}}}, \psi_{\bar{\mathbf{b}}, m} \rangle \sim \mathcal{N}\left(0, \sigma^2 \cdot \frac{2^N}{N^B}\right)$ (98), where the standard deviation can be made arbitrarily small by increasing the number of samples N^B within each band $\bar{\mathbf{b}}$. In Section 6 this fact will be exploited to achieve significantly higher recovery performance for the proposed operator $\mathcal{M}_{\mathbf{H}}^D$ compared to ideal modulo \mathcal{M}_{λ} .

6. Numerical study

Let $\mathbf{V} = [\mathbf{v}_1, \mathbf{v}_2]$ be a randomly generated matrix such that $\|\mathbf{v}_1\|_2 = \|\mathbf{v}_2\|_2 = 1$. The input $f : \mathbb{R}^2 \rightarrow \mathbb{R}$ was restricted to two variables x_1, x_2 for visualisation purposes, and was generated as $f(\mathbf{x}) = f_0(\mathbf{V}\mathbf{x})$, where

$$f_0(x_1, x_2) = \sum_{\mathbf{k} \in \mathbb{Z}^2} c_{\mathbf{k}} \frac{\sin\left(\Omega_1\left(x_1 - k_1 \frac{\pi}{\Omega_1}\right)\right)}{\Omega_1\left(x_1 - k_1 \frac{\pi}{\Omega_1}\right)} \cdot \frac{\sin\left(\Omega_2\left(x_2 - k_2 \frac{\pi}{\Omega_2}\right)\right)}{\Omega_2\left(x_2 - k_2 \frac{\pi}{\Omega_2}\right)}. \quad (53)$$

We selected $\Omega_1 = \Omega_2 = 1$, and computed f for $\mathbf{x} \in [-5, 5]^2$. The coefficients $c_{\mathbf{k}}$ were randomly generated for $|k_1| \leq 1, |k_2| \leq 1$, drawn from the uniform distribution on $[-1, 1]$. The dynamic range of f is $[-1, 1]$. We encoded f using the ideal modulo \mathcal{M}_λ with threshold $\lambda = 0.3$ and the proposed modulo-hysteresis $\mathcal{M}_{\mathbf{H}}^2$ with $\lambda = 0.3, h = 0.19, B = 0.32$. The output samples, computed on lattice Λ with basis vectors $\mathbf{v}_1, \mathbf{v}_2$ and sampling periods T_1, T_2 . We kept $T_1 = 0.02$ s constant because its choice affects in a similar fashion recovery from \mathcal{M}_λ and $\mathcal{M}_{\mathbf{H}}^2$ (see [14]). We varied T_2 in the range $[0.005 \text{ s}, 0.08 \text{ s}]$. The output samples are

$$y_1[\mathbf{k}] = \mathcal{M}_\lambda(f(\mathbf{V}\mathbf{T}\mathbf{k})) + \eta[\mathbf{k}], \quad (54)$$

$$y_2[\mathbf{k}] = \mathcal{M}_{\mathbf{H}}^2 f(\mathbf{V}\mathbf{T}\mathbf{k}) + \eta[\mathbf{k}], \quad (55)$$

where $\eta[\mathbf{k}] \sim \mathcal{N}(0, \sigma^2)$. We varied σ in the range $[0.04, 0.08]$, and recovered the input $\tilde{\gamma}[\mathbf{k}] = f(\mathbf{V}\mathbf{T}\mathbf{k}) + \eta[\mathbf{k}]$ up to a constant multiple of 2λ for \mathcal{M}_λ and $2h$ for $\mathcal{M}_{\mathbf{H}}^2$. We generated 100 random inputs f and 100 noise sequences $\eta[\mathbf{k}]$ and counted the number of inputs correctly reconstructed using each method. In our context, correctly reconstructed means that the recovery conditions hold true. The results are depicted in Fig. 3. We note that, while the accuracy increases significantly for $\mathcal{M}_{\mathbf{H}}^2$ for small T_2 , as proven by Theorem 3, for \mathcal{M}_λ the reverse happens. This is because \mathcal{M}_λ processes the input in a line-by-line fashion, and does not exploit in any way the higher resolution along dimension x_2 . In fact, here a higher resolution simply adds more noise samples from sequence $\eta[\mathbf{k}]$, which are not filtered and thus increase the probability that (52) does not hold. We also note that, for larger sampling periods $T_2 \sim 0.08$ s, \mathcal{M}_λ performs slightly better for low noise, i.e., $\sigma < 0.05$. This is explained by the fact that the

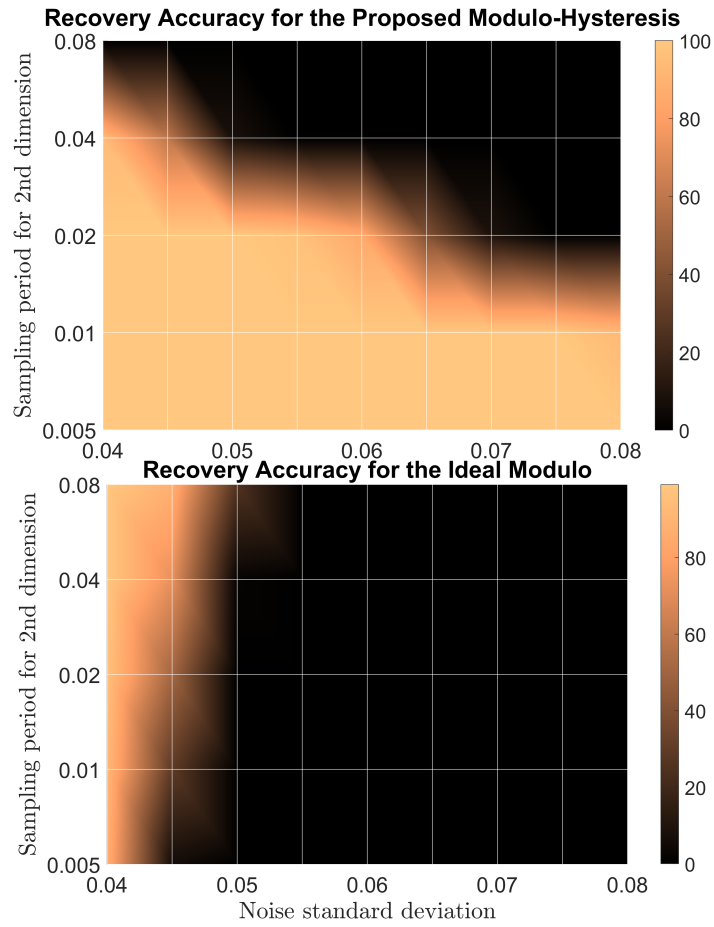


Figure 3: Reconstruction accuracy comparison for (a) the ideal modulo \mathcal{M}_λ and (b) modulo-hysteresis \mathcal{M}_H^D for a two-dimensional input.

modulo-hysteresis requirement $|\langle \eta_{\bar{\mathbf{k}}}, \Delta^N [\cdot - m] \rangle| < h/2 - (T_1 \Omega_1 e)^N \|f\|_\infty$ is more strict than (52) given that $h/2 < \lambda$. This is a small trade-off that enables $\mathcal{M}_{\mathbf{H}}^2$ to handle arbitrarily large values of σ for small enough sampling periods T_2 .

7. Proofs

7.1. Multi-Dimensional Modulo Properties

Proof for Proposition 1 (Bandlimited slices). We consider the slice $f_{\mathbf{V}} = f(\mathbf{V}\mathbf{x})$ along dimension x_d , with $d \in \{1, \dots, D\}$ fixed. To this end, we apply the $(D-1)$ -dimensional inverse Fourier transform to $f_{\mathbf{V}}$ corresponding to all variables apart from x_d , such that

$$\frac{1}{(2\pi)^{D-1}} \int_{\mathbb{R}^{D-1}} \mathcal{F}f_{\mathbf{V}}(\omega) e^{j\langle \omega, \mathbf{x} \rangle} d\omega_1 \dots d\omega_{d-1} d\omega_{d+1} \dots d\omega_D \quad (56)$$

$$= \int_{\mathbb{R}} f_{\mathbf{V}}(\mathbf{x}) e^{-j\omega_d x_d} dx_d \quad (57)$$

$$= \int_{\mathbb{R}} f\left(\sum_{d=1}^D x_d \mathbf{v}_d\right) e^{-j\omega_d x_d} dx_d = \mathcal{F}g_d(\omega_d). \quad (58)$$

Therefore, the spectrum of g_d depends on the spectrum of $f_{\mathbf{V}}(\mathbf{x})$, which will be evaluated in the following. To this end, via the change of variable $\mathbf{x} = \mathbf{V}\mathbf{x}^*$, we get that

$$\begin{aligned} \mathcal{F}f(\omega) &= \int_{\mathbb{R}^D} f(\mathbf{x}) e^{-j\langle \omega, \mathbf{x} \rangle} d\mathbf{x} = \int_{\mathbb{R}^D} f(\mathbf{V}\mathbf{x}^*) e^{-j\langle \omega, \mathbf{V}\mathbf{x}^* \rangle} |\det(\mathbf{V})| d\mathbf{x}^* \\ &= \int_{\mathbb{R}^D} f(\mathbf{V}\mathbf{x}^*) e^{-j\langle \mathbf{V}^\top \omega, \mathbf{x}^* \rangle} |\det(\mathbf{V})| d\mathbf{x}^* \quad (59) \\ &= |\det(\mathbf{V})| \cdot \mathcal{F}f_{\mathbf{V}}(\mathbf{V}^\top \omega). \end{aligned}$$

Using $f \in \text{PW}_\Omega(\mathbb{R}^D)$ we get that $\text{supp}(\mathcal{F}f) \subseteq \mathbf{V}^{-\top} \cdot \prod_{d=1}^D (-\Omega_d, \Omega_d)$. Then, via (59), we have that $\text{supp}(\mathcal{F}f_{\mathbf{V}}) \subseteq \prod_{d=1}^D (-\Omega_d, \Omega_d)$, and therefore $\mathcal{F}f_{\mathbf{V}}(\omega) = 0, \forall \omega_d \in \mathbb{R}, |\omega_d| > \Omega_d$ in (56). It follows that $\mathcal{F}g_d(\omega_d) = 0, \forall \omega_d \in \mathbb{R}, |\omega_d| > \Omega_d, d \neq 1$. Furthermore, choosing $d = 1$ gives us $\mathcal{F}f_{\bar{\mathbf{x}}}(\omega_1) = 0, \forall \omega_1 \in \mathbb{R}, |\omega_1| > \Omega_1$, which finalizes the proof. \square

Proof for Proposition 2 (Folding time separation). We first show an intermediate result in the following lemma.

Lemma 1. For a fixed vector $\bar{\mathbf{b}} \in \mathbb{Z}^{D-1}$ indicating the modulo band and $r \in \{1, \dots, R\}$, let $g_{\bar{\mathbf{x}}, r} : \mathbb{R} \rightarrow \mathbb{R}$ and $g_r : \mathbb{R} \rightarrow \mathbb{R}$ be two functions defined as

$$g_{\bar{\mathbf{x}}, r}(x_1) \triangleq f_{\bar{\mathbf{x}}}(x_1) - \varepsilon_{\bar{\mathbf{b}}, r-1}(x_1), \quad \forall \mathbf{x} \in \mathbb{R}^D, \quad (60)$$

$$g_r(x_1) \triangleq \sup_{\bar{\mathbf{x}} \in \mathcal{R}_{\bar{\mathbf{b}}}} |g_{\bar{\mathbf{x}}, r}(x_1)|, \quad \forall x_1 \in \mathbb{R}. \quad (61)$$

Then $g_{\bar{\mathbf{x}}, r}$ and $|g_{\bar{\mathbf{x}}, r}|$ are Lipschitz-continuous as functions of $\mathbf{x} = [x_1, \bar{\mathbf{x}}] \in \mathbb{Z}^D$ and g_r is Lipschitz-continuous as function of $x_1 \in \mathbb{R}$. Furthermore, the Lipschitz constant in all cases is $\|\boldsymbol{\Omega}\|_2 \cdot \|f\|_\infty$.

Proof. We begin by deriving a bound for the Lipschitz constant of function $f_{\mathbf{V}} = f(\mathbf{V}\cdot)$. Given that f is differentiable, according to the *mean value theorem*

$$f_{\mathbf{V}}(\mathbf{x}) - f_{\mathbf{V}}(\boldsymbol{\chi}) = \langle \nabla f_{\mathbf{V}}(\mathbf{c}), \mathbf{x} - \boldsymbol{\chi} \rangle, \quad \forall \mathbf{x}, \boldsymbol{\chi} \in \mathbb{R}^D, \quad (62)$$

where $\mathbf{c} = \alpha \mathbf{x} + (1 - \alpha) \boldsymbol{\chi}$, $\alpha \in [0, 1]$ is an intermediate point on the segment joining \mathbf{x} and $\boldsymbol{\chi}$. Due to the *Cauchy-Schwartz inequality*

$$|f_{\mathbf{V}}(\mathbf{x}) - f_{\mathbf{V}}(\boldsymbol{\chi})| \leq \|\nabla f_{\mathbf{V}}(\mathbf{c})\|_2 \cdot \|\mathbf{x} - \boldsymbol{\chi}\|_2. \quad (63)$$

Next, we use the Bernštein bounds in (15) to derive a bound for $\|\nabla f_{\mathbf{V}}\|$ as follows

$$\|\nabla f_{\mathbf{V}}\|_2^2 = \sum_{d=1}^D \left| \frac{\partial}{\partial x_d} f_{\mathbf{V}}(\mathbf{c}) \right|^2 \leq \sum_{d=1}^D \Omega_d^2 \|f\|_\infty^2 \quad (64)$$

which means $f_{\mathbf{V}}$ is a Lipschitz-continuous function satisfying

$$|f_{\mathbf{V}}(\mathbf{x}) - f_{\mathbf{V}}(\boldsymbol{\chi})| \leq \|\boldsymbol{\Omega}\|_2 \cdot \|f\|_\infty \cdot \|\mathbf{x} - \boldsymbol{\chi}\|_2, \quad \forall \mathbf{x}, \boldsymbol{\chi} \in \mathbb{R}^D. \quad (65)$$

For all $\bar{\mathbf{x}}, \bar{\boldsymbol{\chi}} \in \mathbb{R}^{D-1}$ and $\forall x_1, \chi_1 > \tau_{\bar{\mathbf{b}}, r-1}$ we have $\varepsilon_{\bar{\mathbf{b}}, r-1}(x_1) = \varepsilon_{\bar{\mathbf{b}}, r-1}(\chi_1)$, which implies

$$\begin{aligned} \left| |g_{\bar{\mathbf{x}}, r}(x_1)| - |g_{\bar{\boldsymbol{\chi}}, r}(\chi_1)| \right| &\leq \left| g_{\bar{\mathbf{x}}, r}(x_1) - g_{\bar{\boldsymbol{\chi}}, r}(\chi_1) \right| = \left| f_{\bar{\mathbf{x}}}(x_1) - f_{\bar{\boldsymbol{\chi}}}(\chi_1) \right| \\ &= |f_{\mathbf{V}}(\mathbf{x}) - f_{\mathbf{V}}(\boldsymbol{\chi})| \leq \|\boldsymbol{\Omega}\|_2 \cdot \|f\|_\infty \cdot \|\mathbf{x} - \boldsymbol{\chi}\|_2. \end{aligned} \quad (66)$$

The final step is to show that $g_r(x_1)$ is also Lipschitz, i.e., that the supremum does not change the Lipschitz constant. To this end, we note the following two properties of the

supremum. Specifically, for $\forall \epsilon > 0$ and $\forall x_1, \chi_1 \in \mathbb{R}$, $\exists \bar{x}_\epsilon, \bar{\chi}_\epsilon \in \mathcal{R}_{\bar{\mathbf{b}}}$ such that

$$\begin{aligned} \left| g_{\bar{\chi}_\epsilon}(x_1) \right| &\leq g_r(x_1) < |g_{\bar{x}_\epsilon}(x_1)| + \epsilon, \\ |g_{\bar{x}_\epsilon}(\chi_1)| &\leq g_r(\chi_1) < \left| g_{\bar{\chi}_\epsilon}(\chi_1) \right| + \epsilon. \end{aligned} \quad (67)$$

We derive that $g_r(x_1) - g_r(\chi_1) \leq |g_{\bar{x}_\epsilon}(x_1)| + \epsilon - |g_{\bar{x}_\epsilon}(\chi_1)|$. Similarly, we get $g_r(\chi_1) - g_r(x_1) \leq \left| g_{\bar{\chi}_\epsilon}(\chi_1) \right| + \epsilon - \left| g_{\bar{\chi}_\epsilon}(x_1) \right|$. Finally, we restrict x_1, χ_1 in (67) to satisfy $x_1, \chi_1 > \tau_{\bar{\mathbf{b}}, r-1}$ and select $\bar{x}, \bar{\chi}$ in (66) as $\bar{x} = \bar{x}_\epsilon, \bar{\chi} = \bar{\chi}_\epsilon$, which yields

$$\begin{aligned} |g_r(x_1) - g_r(\chi_1)| &\leq \max \left\{ |g_{\bar{x}_\epsilon}(x_1)| - |g_{\bar{x}_\epsilon}(\chi_1)|, \left| g_{\bar{\chi}_\epsilon}(\chi_1) \right| - \left| g_{\bar{\chi}_\epsilon}(x_1) \right| \right\} + \epsilon \\ &\leq \max \left\{ \left| |g_{\bar{x}_\epsilon}(x_1)| - |g_{\bar{x}_\epsilon}(\chi_1)| \right|, \left| \left| g_{\bar{\chi}_\epsilon}(\chi_1) \right| - \left| g_{\bar{\chi}_\epsilon}(x_1) \right| \right| \right\} + \epsilon \\ &\leq |\Omega_1| \cdot \|f\|_\infty \cdot |x_1 - \chi_1| + \epsilon, \quad \forall \epsilon > 0. \end{aligned}$$

Taking $\epsilon \rightarrow 0$ above proves the required result. \square

We begin by evaluating $g_{\bar{x},1}(\tau_{\bar{\mathbf{b}},0})$

$$g_{\bar{x},1}(\tau_{\bar{\mathbf{b}},0}) = f_{\bar{x}}(\tau_{\bar{\mathbf{b}},0}) - hM_{\bar{\mathbf{b}}} = f_{\bar{x}}(\tau_{\bar{\mathbf{b}},0}) - h \left[\frac{\inf_{\bar{\chi} \in \mathcal{R}_{\bar{\mathbf{b}}}} f_{\bar{\chi}}(\tau_{\bar{\mathbf{b}},0}) + \lambda}{h} \right] + h. \quad (68)$$

Using that $x - 1 < \lfloor x \rfloor \leq x$ we derive

$$\begin{aligned} \inf_{\bar{x} \in \mathcal{R}_{\bar{\mathbf{b}}}} g_{\bar{x},1}(\tau_{\bar{\mathbf{b}},0}) &\geq \inf_{\bar{x} \in \mathcal{R}_{\bar{\mathbf{b}}}} \left[f_{\bar{x}}(\tau_{\bar{\mathbf{b}},0}) - h \frac{\inf_{\bar{\chi} \in \mathcal{R}_{\bar{\mathbf{b}}}} f_{\bar{\chi}}(\tau_{\bar{\mathbf{b}},0}) + \lambda}{h} + h \right] \\ &= -\lambda + h \\ \sup_{\bar{x} \in \mathcal{R}_{\bar{\mathbf{b}}}} g_{\bar{x},1}(\tau_{\bar{\mathbf{b}},0}) &\leq \sup_{\bar{x} \in \mathcal{R}_{\bar{\mathbf{b}}}} \left[f_{\bar{x}}(\tau_{\bar{\mathbf{b}},0}) - h \frac{\inf_{\bar{\chi} \in \mathcal{R}_{\bar{\mathbf{b}}}} f_{\bar{\chi}}(\tau_{\bar{\mathbf{b}},0}) + \lambda}{h} + 2h \right] \\ &\leq -\lambda + 2h + \mathcal{D}f \leq \lambda - h. \end{aligned} \quad (69)$$

Then, given that

$$g_1(\tau_{\bar{\mathbf{b}},0}) = \sup_{\bar{x} \in \mathcal{R}_{\bar{\mathbf{b}}}} |g_{\bar{x},1}(\tau_{\bar{\mathbf{b}},0})| = \max \left\{ \sup_{\bar{x} \in \mathcal{R}_{\bar{\mathbf{b}}}} g_{\bar{x},1}(\tau_{\bar{\mathbf{b}},0}), - \inf_{\bar{x} \in \mathcal{R}_{\bar{\mathbf{b}}}} g_{\bar{x},1}(\tau_{\bar{\mathbf{b}},0}) \right\},$$

we get $g_1(\tau_{\bar{\mathbf{b}},0}) \leq \lambda - h$. Furthermore, g_1 is Lipschitz-continuous due to Lemma 1, and therefore continuous. Thus, given that $\tau_{\bar{\mathbf{b}},1} = \inf \{x_1 > \tau_{\bar{\mathbf{b}},0} | g_1(x_1) = \lambda\}$ is true by definition, we get $g_1(\tau_{\bar{\mathbf{b}},1}) = \lambda$.

We then investigate the variation of function g_1 between folding times $\tau_{\bar{\mathbf{b}},0}$ and $\tau_{\bar{\mathbf{b}},1}$ as follows. Using Lemma 1, we get

$$g_1(\tau_{\bar{\mathbf{b}},0}) - g_1(\tau_{\bar{\mathbf{b}},1}) \leq \Omega_1 \|f\|_\infty \cdot |\tau_{\bar{\mathbf{b}},1} - \tau_{\bar{\mathbf{b}},0}|,$$

and then we use that $g_1(\tau_{\bar{\mathbf{b}},1}) = \lambda$ and $g_1(\tau_{\bar{\mathbf{b}},0}) < \lambda - h$ to derive

$$h \leq |g_1(\tau_{\bar{\mathbf{b}},0}) - g_1(\tau_{\bar{\mathbf{b}},1})|.$$

Therefore the folding times satisfy the following bound

$$|\tau_{\bar{\mathbf{b}},1} - \tau_{\bar{\mathbf{b}},0}| \geq \frac{h}{\Omega_1 \|f\|_\infty}. \quad (70)$$

We note the resemblance between (70) the one-dimensional case (8). Next, we will show by induction that $g_r(\tau_{\bar{\mathbf{b}},r-1}) \leq \lambda - h$, $g_r(\tau_{\bar{\mathbf{b}},r}) = \lambda$ and then $|\tau_{\bar{\mathbf{b}},r} - \tau_{\bar{\mathbf{b}},r-1}| \geq \frac{h}{\Omega_1 \|f\|_\infty}$ holds where sequence $\{\tau_{\bar{\mathbf{b}},1}, \dots, \tau_{\bar{\mathbf{b}},r}\}$ is computed according to (22). The *base case* $r = 1$ is shown in the derivation to (70). For the *induction step* we proceed with computing $g_{r+1}(\tau_{\bar{\mathbf{b}},r})$.

$$g_{r+1}(\tau_{\bar{\mathbf{b}},r}) = \sup_{\bar{\mathbf{x}} \in \mathcal{R}_{\bar{\mathbf{b}}}} |g_{\bar{\mathbf{x}},r+1}(\tau_{\bar{\mathbf{b}},r})| = \sup_{\bar{\mathbf{x}} \in \mathcal{R}_{\bar{\mathbf{b}}}} |f_{\bar{\mathbf{x}}}(\tau_{\bar{\mathbf{b}},r}) - \varepsilon_{\bar{\mathbf{b}},r}(\tau_{\bar{\mathbf{b}},r})| \quad (71)$$

$$= \sup_{\bar{\mathbf{x}} \in \mathcal{R}_{\bar{\mathbf{b}}}} \left| f_{\bar{\mathbf{x}}}(\tau_{\bar{\mathbf{b}},r}) - \varepsilon_{\bar{\mathbf{b}},r-1}(\tau_{\bar{\mathbf{b}},r}) + h s_{\bar{\mathbf{b}},r} \mathbb{1}_{[\tau_{\bar{\mathbf{b}},r}, \infty)}(\tau_{\bar{\mathbf{b}},r}) \right| \quad (72)$$

$$= \sup_{\bar{\mathbf{x}} \in \mathcal{R}_{\bar{\mathbf{b}}}} |g_{\bar{\mathbf{x}},r}(\tau_{\bar{\mathbf{b}},r}) - h s_{\bar{\mathbf{b}},r}|, \text{ where } s_{\bar{\mathbf{b}},r} = \text{sign}[g_{\bar{\mathbf{b}}B,r}(\tau_{\bar{\mathbf{b}},r})]. \quad (73)$$

We have that $\sup_{\bar{\mathbf{x}} \in \mathcal{R}_{\bar{\mathbf{b}}}} |g_{\bar{\mathbf{x}},r}(\tau_{\bar{\mathbf{b}},r})| = \lambda$, which leads to two possible cases

1. $\sup_{\bar{\mathbf{x}} \in \mathcal{R}_{\bar{\mathbf{b}}}} |g_{\bar{\mathbf{x}},r}(\tau_{\bar{\mathbf{b}},r})| = \sup_{\bar{\mathbf{x}} \in \mathcal{R}_{\bar{\mathbf{b}}}} g_{\bar{\mathbf{x}},r}(\tau_{\bar{\mathbf{b}},r}) = \lambda$

Here we use that

$$\sup_{\bar{\mathbf{x}} \in \mathcal{R}_{\bar{\mathbf{b}}}} g_{\bar{\mathbf{x}},r}(\tau_{\bar{\mathbf{b}},r}) - \inf_{\bar{\mathbf{x}} \in \mathcal{R}_{\bar{\mathbf{b}}}} g_{\bar{\mathbf{x}},r}(\tau_{\bar{\mathbf{b}},r}) = \sup_{\bar{\mathbf{x}} \in \mathcal{R}_{\bar{\mathbf{b}}}} f_{\bar{\mathbf{x}}}(\tau_{\bar{\mathbf{b}},r}) - \inf_{\bar{\mathbf{x}} \in \mathcal{R}_{\bar{\mathbf{b}}}} f_{\bar{\mathbf{x}}}(\tau_{\bar{\mathbf{b}},r}) < \mathcal{D}f,$$

which then implies $\inf_{\bar{\mathbf{x}} \in \mathcal{R}_{\bar{\mathbf{b}}}} g_{\bar{\mathbf{x}},r}(\tau_{\bar{\mathbf{b}},r}) > \lambda - \mathcal{D}f > \lambda - h/2 > 0$. Then

$$\text{sign}[g_{\bar{\mathbf{x}},r}(\tau_{\bar{\mathbf{b}},r})] = s_{\bar{\mathbf{b}},r} = \text{sign}[g_{\bar{\mathbf{b}}B,r}(\tau_{\bar{\mathbf{b}},r})] = 1.$$

Then, continuing the derivation in (73), we get

$$g_{r+1}(\tau_{\bar{\mathbf{b}},r}) = \sup_{\bar{\mathbf{x}} \in \mathcal{R}_{\bar{\mathbf{b}}}} |g_{\bar{\mathbf{x}},r}(\tau_{\bar{\mathbf{b}},r}) - h s_{\bar{\mathbf{b}},r}| = \sup_{\bar{\mathbf{x}} \in \mathcal{R}_{\bar{\mathbf{b}}}} |g_{\bar{\mathbf{x}},r}(\tau_{\bar{\mathbf{b}},r}) - h|. \quad (74)$$

Next, we evaluate the sign of $g_{\bar{x},r}(\tau_{\bar{\mathbf{b}},r}) - h$ as follows

$$g_{\bar{x},r}(\tau_{\bar{\mathbf{b}},r}) - h \leq \sup_{\bar{x} \in \mathcal{R}_{\bar{\mathbf{b}}}} g_{\bar{x},r}(\tau_{\bar{\mathbf{b}},r}) - h = \lambda - h, \quad (75)$$

$$g_{\bar{x},r}(\tau_{\bar{\mathbf{b}},r}) - h \geq \inf_{\bar{x} \in \mathcal{R}_{\bar{\mathbf{b}}}} g_{\bar{x},r}(\tau_{\bar{\mathbf{b}},r}) - h = \lambda - \mathcal{D}f - h \quad (76)$$

$$\geq \lambda - \frac{3h}{2} > 0. \quad (77)$$

The final inequality follows from the assumption $h < 2\lambda/3$. It follows that (74)

$$g_{r+1}(\tau_{\bar{\mathbf{b}},r}) = \sup_{\bar{x} \in \mathcal{R}_{\bar{\mathbf{b}}}} g_{\bar{x},r}(\tau_{\bar{\mathbf{b}},r}) - h \leq \lambda - h. \quad (78)$$

2. $\sup_{\bar{x} \in \mathcal{R}_{\bar{\mathbf{b}}}} |g_{\bar{x},r}(\tau_{\bar{\mathbf{b}},r})| = -\inf_{\bar{x} \in \mathcal{R}_{\bar{\mathbf{b}}}} g_{\bar{x},r}(\tau_{\bar{\mathbf{b}},r}) = \lambda$. As before, here we prove that $\text{sign}[g_{\bar{x},r}(\tau_{\bar{\mathbf{b}},r})] = -1$, $g_{r+1}(\tau_{\bar{\mathbf{b}},r}) = \sup_{\bar{x} \in \mathcal{R}_{\bar{\mathbf{b}}}} |g_{\bar{x},r}(\tau_{\bar{\mathbf{b}},r}) + h|$, and finally $g_{\bar{x},r}(\tau_{\bar{\mathbf{b}},r}) + h \in [-\lambda + h, 0)$ which leads to (78).

As in the *base case* $r = 1$, given that $\tau_{\bar{\mathbf{b}},r+1} = \inf \{x_1 > \tau_{\bar{\mathbf{b}},r} | g_{r+1}(x_1) = \lambda\}$ is true by definition and using the continuity of g_{r+1} , we get $g_{r+1}(\tau_{\bar{\mathbf{b}},r+1}) = \lambda$. Using (78) and the same reasoning as in the *base case* leading to (70) the proposition follows. \square

Proof for Proposition 3 (Well-defined operator). For this to be true we need to show the existence of $R_{\bar{\mathbf{b}}}^+$ in (25). First, we derive some preliminary properties of $f_{\bar{x}}$. Due to Proposition 1 we have that $f_{\bar{x}} \in \text{PW}_{\Omega_1}(\mathbb{R})$ and implicitly $f_{\bar{x}} \in L^2(\mathbb{R})$. Using the properties of the $\text{PW}_{\Omega}(\mathbb{R}^D)$ space and $\|f\|_{\infty} < \infty$, it follows that

$$\lim_{x_1 \rightarrow \infty} f_{\bar{x}}(x_1) = 0, \quad \forall \bar{x} \in \mathbb{R}^{D-1}. \quad (79)$$

We require to show that the limit in (79) is uniform for all \bar{x} , which is done in the following lemma.

Lemma 2 (Uniform convergence). *The following holds true*

$$\forall \epsilon > 0, \exists x_1^* > 0, \forall x_1 > x_1^*, \forall \bar{x} \in \mathcal{R}_{\bar{\mathbf{b}}}, \quad \text{s.t.} \quad |f_{\bar{x}}(x_1)| < \epsilon.$$

Proof. We prove by contradiction. Thus we assume

$$\exists \epsilon > 0, \forall x_1^* > 0, \exists x_1 > x_1^*, \exists \bar{x} \in \mathcal{R}_{\bar{\mathbf{b}}}, \quad \text{s.t.} \quad |f_{\bar{x}}(x_1)| \geq \epsilon.$$

We select $x_1^* = n, x_1 = x_{1,n}, \bar{x} = \bar{x}_n \in \mathcal{R}_{\bar{\mathbf{b}}}$ which leads to

$$\exists \epsilon > 0, \forall n \in \mathbb{N}^*, \exists x_{1,n} > n, \exists \bar{x}_n \in \mathcal{R}_{\bar{\mathbf{b}}}, \quad \text{s.t.} \quad |f_{\bar{x}_n}(x_{1,n})| \geq \epsilon. \quad (80)$$

We use that, because $\mathcal{R}_{\bar{\mathbf{b}}}$ is bounded, then any sequence $\bar{x}_n \in \mathcal{R}_{\bar{\mathbf{b}}}$ has a subsequence $\bar{x}_{\kappa_m} \in \mathcal{R}_{\bar{\mathbf{b}}}$ that converges to a point in the closure of $\mathcal{R}_{\bar{\mathbf{b}}}$, i.e.,

$$\lim_{m \rightarrow \infty} \bar{x}_{\kappa_m} = \bar{x}_\infty \in \text{cl}(\mathcal{R}_{\bar{\mathbf{b}}}).$$

We then select $n = \kappa_m$ in (80) and get

$$\exists \epsilon > 0, \forall m \in \mathbb{N}^*, \exists x_{1,\kappa_m} > \kappa_m, \exists \bar{x}_{\kappa_m} \in \mathcal{R}_{\bar{\mathbf{b}}}, \quad \text{s.t.} \quad |f_{\bar{x}_{\kappa_m}}(x_{1,\kappa_m})| \geq \epsilon.$$

Furthermore, f is a Lipschitz-continuous function with constant $\|\Omega\|_2 \cdot \|f\|_\infty$ as shown in (65), which implies that

$$\begin{aligned} |f_{\bar{x}_{\kappa_m}}(x_{1,\kappa_m})| - |f_{\bar{x}_\infty}(x_{1,\kappa_m})| &\leq |f_{\bar{x}_{\kappa_m}}(x_{1,\kappa_m}) - f_{\bar{x}_\infty}(x_{1,\kappa_m})| \\ &\leq \|\Omega\|_2 \cdot \|f\|_\infty \cdot \|\bar{x}_{\kappa_m} - \bar{x}_\infty\|_2. \end{aligned}$$

This allows defining the following lower bound on $|f_{\bar{x}_\infty}(x_{1,\kappa_m})|$

$$|f_{\bar{x}_\infty}(x_{1,\kappa_m})| \geq |f_{\bar{x}_{\kappa_m}}(x_{1,\kappa_m})| - \|\Omega\|_2 \cdot \|f\|_\infty \cdot \|\bar{x}_{\kappa_m} - \bar{x}_\infty\|_2.$$

We know that $|f_{\bar{x}_{\kappa_m}}(x_{1,\kappa_m})| \geq \epsilon$ and $\lim_{m \rightarrow \infty} \|\bar{x}_{\kappa_m} - \bar{x}_\infty\|_2 = 0$. Then it follows that $|f_{\bar{x}_\infty}(x_{1,\kappa_m})|$ cannot converge to 0 for $m \rightarrow \infty$, which directly contradicts (79). Then the starting assumption is wrong, and the Lemma follows. \square

We approach this proof by contradiction. If we assume that $R_{\bar{\mathbf{b}}}^+ \geq 0$ does not exist it follows that $\tau_{\bar{\mathbf{b}},r}$ in (22) is well-defined for $r \in \mathbb{Z}_+$. Given that, by definition, $\tau_{\bar{\mathbf{b}},r}$ is increasing as a function of r , then due to Proposition 2 it follows that $\lim_{r \rightarrow \infty} \tau_{\bar{\mathbf{b}},r} = \infty$. We use Lemma 2 for $\epsilon = \frac{h}{4}$, which yields $\exists x_1^* > 0$ such that $|f_{\bar{x}}(x_1)| < \frac{h}{4}, \forall \bar{x} \in \mathcal{R}_{\bar{\mathbf{b}}}, \forall x_1 > x_1^*$. Given our assumption on $\tau_{\bar{\mathbf{b}},r}$ then $\exists r^* \in \mathbb{Z}_+$ such that $\tau_{\bar{\mathbf{b}},r^*} > x_1^*$. Thus, by definition, $\sup_{\bar{x} \in \mathcal{R}_{\bar{\mathbf{b}}}} |f_{\bar{x}}(\tau_{\bar{\mathbf{b}},r^*}) - \varepsilon_{\bar{\mathbf{b}},r^*}(\tau_{\bar{\mathbf{b}},r^*})| = \lambda$. Using (73)–(78) where r is replaced by r^* and functions $g_r, g_{\bar{x},r}$ are defined in (60),(61), one can show that $g_{r^*+1}(\tau_{\bar{\mathbf{b}},r^*}) \leq \lambda - h$. The next folding time $\tau_{\bar{\mathbf{b}},r^*+1}$ satisfies $g_{r^*+1}(\tau_{\bar{\mathbf{b}},r^*+1}) = \lambda$.

In the following we will show this is not possible. Specifically, for $x_1 > \tau_{\bar{\mathbf{b}}, r^*}$,

$$\begin{aligned}
g_{r^*+1}(x_1) &= \sup |f_{\bar{\mathbf{x}}}(x_1) - \varepsilon_{\bar{\mathbf{b}}, r^*}(x_1)| = \sup |f_{\bar{\mathbf{x}}}(x_1) - \varepsilon_{\bar{\mathbf{b}}, r^*}(\tau_{\bar{\mathbf{b}}, r^*})| \\
&= \sup |f_{\bar{\mathbf{x}}}(\tau_{\bar{\mathbf{b}}, r^*}) - \varepsilon_{\bar{\mathbf{b}}, r^*}(\tau_{\bar{\mathbf{b}}, r^*}) + f_{\bar{\mathbf{x}}}(x_1) - f_{\bar{\mathbf{x}}}(\tau_{\bar{\mathbf{b}}, r^*})| \\
&\leq \sup |f_{\bar{\mathbf{x}}}(\tau_{\bar{\mathbf{b}}, r^*}) - \varepsilon_{\bar{\mathbf{b}}, r^*}(\tau_{\bar{\mathbf{b}}, r^*})| + \sup |f_{\bar{\mathbf{x}}}(x_1) - f_{\bar{\mathbf{x}}}(\tau_{\bar{\mathbf{b}}, r^*})| \\
&\leq \lambda - h + h/2 = \lambda - h/2 < \lambda.
\end{aligned}$$

We conclude that the definition of $\tau_{\bar{\mathbf{b}}, r^*+1}$ via (22) is therefore not possible, and thus our assumption that $\tau_{\bar{\mathbf{b}}, r}$ is well-defined for $r \in \mathbb{Z}$ is false, and the proposition follows. \square

Proof for Proposition 4 (Modulo output dynamic range). We first assume that x_1 satisfies $x_1 \in [\tau_{\bar{\mathbf{b}}, r}, \tau_{\bar{\mathbf{b}}, r+1})$ and then extrapolate to the whole real axis. Given the definition of function $\varepsilon_{\bar{\mathbf{b}}, r}$ (24) it follows that $\varepsilon(\mathbf{V}\mathbf{x}) = \varepsilon_{\bar{\mathbf{b}}, r}(x_1)$ and thus

$$z(\mathbf{V}\mathbf{x}) = f_{\bar{\mathbf{x}}}(x_1) - \varepsilon_{\bar{\mathbf{b}}, r}(x_1) = g_{\bar{\mathbf{x}}, r+1}(x_1).$$

It was shown before that $g_{\bar{\mathbf{x}}, r+1}(\tau_{\bar{\mathbf{b}}, r}) \leq \lambda - h$ (78). Furthermore, due to the definition of $\tau_{\bar{\mathbf{b}}, r+1}$ (22) we get that $g_{r+1}(\tau_{\bar{\mathbf{b}}, r+1}) = \lambda$ and $|g_{\bar{\mathbf{x}}, r+1}(x_1)| < \lambda$ when our assumption $x_1 \in [\tau_{\bar{\mathbf{b}}, r}, \tau_{\bar{\mathbf{b}}, r+1})$ holds. By repeating the process above for $r \in \mathbb{Z}_+$ we get $|z(\mathbf{V}\mathbf{x})| < \lambda, \forall x_1 \geq 0$. For $x_1 < 0$, the process above is reproduced for $x_1 \in (\tau_{\bar{\mathbf{b}}, r-1}, \tau_{\bar{\mathbf{b}}, r}]$, $\forall r \in \mathbb{Z}_-$. \square

Proof for Corollary 1 (Bound for intra-band variation). Let $\mathbf{x}, \chi \in \mathcal{R}_{\bar{\mathbf{b}}}$. As shown before (65), $f_{\mathbf{V}} = f(\mathbf{V}\cdot)$ is a Lipschitz-continuous function with constant $\|\Omega\|_2 \cdot \|f\|_\infty$. Then it follows that

$$|f(\mathbf{V}\mathbf{x}) - f(\mathbf{V}\chi)| \leq \|\Omega\|_2 \cdot \|f\|_\infty \cdot \|\mathbf{x} - \chi\|_2 \quad (81)$$

$$\leq \|\Omega\|_2 \cdot \|f\|_\infty \cdot B\sqrt{D}. \quad (82)$$

We recall that $\mathcal{D}f$ satisfies (26)

$$\mathcal{D}f \triangleq \sup_{\bar{\mathbf{b}} \in \mathbb{Z}^{D-1}, x_1 \in \mathbb{R}} \left[\sup_{\bar{\mathbf{x}} \in \mathcal{R}_{\bar{\mathbf{b}}}} f_{\bar{\mathbf{x}}}(x_1) - \inf_{\bar{\mathbf{x}} \in \mathcal{R}_{\bar{\mathbf{b}}}} f_{\bar{\mathbf{x}}}(x_1) \right]. \quad (83)$$

We fix a $\bar{\mathbf{b}} \in \mathbb{Z}^{D-1}$, and define $\mathcal{D}_{\bar{\mathbf{b}}}f$ as

$$\mathcal{D}_{\bar{\mathbf{b}}}f \triangleq \sup_{x_1 \in \mathbb{R}} \left[\sup_{\bar{\mathbf{x}} \in \mathcal{R}_{\bar{\mathbf{b}}}} f_{\bar{\mathbf{x}}}(x_1) - \inf_{\bar{\mathbf{x}} \in \mathcal{R}_{\bar{\mathbf{b}}}} f_{\bar{\mathbf{x}}}(x_1) \right]. \quad (84)$$

We then use the property that there always exists a sequence in a set converging to the infimum or supremum. Therefore, $\exists \bar{\mathbf{x}}_n, \bar{\mathbf{x}}_n, x_{1,n}$ such that

$$\lim_{n \rightarrow \infty} f_{\bar{\mathbf{x}}_n}(x_{1,n}) - f_{\bar{\mathbf{x}}_n}(x_{1,n}) = \mathcal{D}_{\bar{\mathbf{b}}}f. \quad (85)$$

Given that $f_{\bar{\mathbf{x}}_n}(x_{1,n})$ converges to the supremum and $f_{\bar{\mathbf{x}}_n}(x_{1,n})$ to the infimum, it follows that $\exists N \in \mathbb{Z}_+$ such that $f_{\bar{\mathbf{x}}_n}(x_{1,n}) - f_{\bar{\mathbf{x}}_n}(x_{1,n}) \geq 0, \forall n \in \mathbb{Z}, n \geq N$. Then

$$f_{\bar{\mathbf{x}}_n}(x_{1,n}) - f_{\bar{\mathbf{x}}_n}(x_{1,n}) = \left| f_{\bar{\mathbf{x}}_n}(x_{1,n}) - f_{\bar{\mathbf{x}}_n}(x_{1,n}) \right|, \quad \forall n \geq N \quad (86)$$

$$\leq \|f\|_{\infty} \cdot B\sqrt{D} \cdot \sqrt{\sum_{d=1}^D \Omega_d^2}. \quad (87)$$

By taking $n \rightarrow \infty$ above we have that $\mathcal{D}_{\bar{\mathbf{b}}}f \leq \|f\|_{\infty} \cdot B\sqrt{D} \cdot \sqrt{\sum_{d=1}^D \Omega_d^2}, \forall \bar{\mathbf{b}} \in \mathbb{Z}^{D-1}$, and computing $\mathcal{D}f = \sup_{\bar{\mathbf{b}} \in \mathbb{Z}^{D-1}} \mathcal{D}_{\bar{\mathbf{b}}}f$ leads to the desired bound. \square

7.2. Multi-Dimensional Modulo Recovery

Proof for Proposition 6 (Detection of folding times). As in the continuous-time scenario, we denote the one-dimensional slices of the samples in each band $\bar{\mathbf{b}}$ by

$$\gamma_{\bar{\mathbf{k}}}[k_1] = \gamma \left[k_1 T_1 \mathbf{v}_1 + \sum_{d=2}^D k_d T_d \mathbf{v}_d \right], \quad (88)$$

$$\varepsilon_{\gamma, \bar{\mathbf{k}}}[k_1] = \varepsilon_{\gamma} \left[k_1 T_1 \mathbf{v}_1 + \sum_{d=2}^D k_d T_d \mathbf{v}_d \right], \quad (89)$$

$$\eta_{\bar{\mathbf{k}}}[k_1] = \eta \left[k_1 T_1 \mathbf{v}_1 + \sum_{d=2}^D k_d T_d \mathbf{v}_d \right]. \quad (90)$$

where $\bar{\mathbf{T}}\bar{\mathbf{k}} \in \mathcal{R}_{\bar{\mathbf{b}}}$ and $\bar{\mathbf{k}} = [k_2, \dots, k_D] \in \mathbb{Z}^{D-1}$. We note that, due to Definition 2, $\varepsilon_{\gamma, \bar{\mathbf{k}}}[k_1]$ does not change with $\bar{\mathbf{k}}$ as long as $\bar{\mathbf{T}}\bar{\mathbf{k}} \in \mathcal{R}_{\bar{\mathbf{b}}}$. The filtered samples $y_{\bar{\mathbf{b}}, m}$ satisfy

$$y_{\bar{\mathbf{b}}, m} = \langle y, \psi_{\bar{\mathbf{b}}, m} \rangle = \langle \gamma, \psi_{\bar{\mathbf{b}}, m} \rangle - \langle \varepsilon_{\gamma}, \psi_{\bar{\mathbf{b}}, m} \rangle + \langle \eta, \psi_{\bar{\mathbf{b}}, m} \rangle$$

We first exploit that $\gamma_{\bar{\mathbf{k}}} [k_1] = f_{\bar{\mathbf{T}}\bar{\mathbf{k}}} (k_1 T_1)$ where $f_{\bar{\mathbf{x}}}$ is bandlimited to Ω_1 rad/s, which yields [12, 14]

$$\begin{aligned}
|\langle \gamma, \psi_{\bar{\mathbf{b}}, m} \rangle| &= \left| \frac{1}{N^B} \sum_{\bar{\mathbf{T}}\bar{\mathbf{k}} \in \mathcal{R}_{\bar{\mathbf{b}}}} \langle \gamma_{\bar{\mathbf{k}}}, \Delta^N [\cdot - m] \rangle \right| \\
&\leq \frac{1}{N^B} \sum_{\bar{\mathbf{T}}\bar{\mathbf{k}} \in \mathcal{R}_{\bar{\mathbf{b}}}} |\langle \gamma_{\bar{\mathbf{k}}}, \Delta^N [\cdot - m] \rangle| \\
&\leq \frac{1}{N^B} \sum_{\bar{\mathbf{T}}\bar{\mathbf{k}} \in \mathcal{R}_{\bar{\mathbf{b}}}} (T_1 \Omega_1 e)^N \|f\|_\infty = (T_1 \Omega_1 e)^N \|f\|_\infty.
\end{aligned} \tag{91}$$

Similarly, for the residual samples ε_γ the following holds

$$\begin{aligned}
|\langle \varepsilon_\gamma, \psi_{\bar{\mathbf{b}}, m} \rangle| &= \left| \frac{1}{N^B} \sum_{\bar{\mathbf{T}}\bar{\mathbf{k}} \in \mathcal{R}_{\bar{\mathbf{b}}}} \langle \varepsilon_{\gamma, \bar{\mathbf{k}}}, \Delta^N [\cdot - m] \rangle \right| \\
&\leq \frac{1}{N^B} \sum_{\bar{\mathbf{T}}\bar{\mathbf{k}} \in \mathcal{R}_{\bar{\mathbf{b}}}} |\langle \varepsilon_{\gamma, \bar{\mathbf{k}}}, \Delta^N [\cdot - m] \rangle| = |\langle \varepsilon_{\gamma, \bar{\mathbf{k}}^*}, \Delta^N [\cdot - m] \rangle|,
\end{aligned} \tag{92}$$

for all $\bar{\mathbf{k}}^*$ satisfying $\bar{\mathbf{T}}\bar{\mathbf{k}}^* \in \mathcal{R}_{\bar{\mathbf{b}}}$, given that $\varepsilon_{\gamma, \bar{\mathbf{k}}}$ does not change within the band $\bar{\mathbf{b}}$ as a function of $\bar{\mathbf{k}}$ (24). We note that $\text{supp} (\Delta^N [\cdot - m]) = \{m, \dots, m + N\}$ and derive that

$$\begin{cases} |\langle \varepsilon_\gamma, \psi_{\bar{\mathbf{b}}, m} \rangle| \geq h & \text{if } m \in \mathbb{S}_N, \\ |\langle \varepsilon_\gamma, \psi_{\bar{\mathbf{b}}, m} \rangle| = 0 & \text{otherwise,} \end{cases} \tag{93}$$

Therefore, if $(T_1 \Omega_1 e)^N \|f\|_\infty < h/2$ and $|\langle \eta, \psi_{\bar{\mathbf{b}}, m} \rangle| < h/2 - (T_1 \Omega_1 e)^N \|f\|_\infty$, then, if $m \in \mathbb{S}_N$,

$$\begin{aligned}
|\langle y, \psi_{\bar{\mathbf{b}}, m} \rangle| &= |\langle \varepsilon_\gamma, \psi_{\bar{\mathbf{b}}, m} \rangle - (\langle \gamma, \psi_{\bar{\mathbf{b}}, m} \rangle + \langle \eta, \psi_{\bar{\mathbf{b}}, m} \rangle)| \\
&\geq |\langle \varepsilon_\gamma, \psi_{\bar{\mathbf{b}}, m} \rangle| - |\langle \gamma, \psi_{\bar{\mathbf{b}}, m} \rangle + \langle \eta, \psi_{\bar{\mathbf{b}}, m} \rangle| \\
&\geq h - h/2 = h/2.
\end{aligned} \tag{94}$$

Furthermore, for $m \notin \mathbb{S}_N$, we get $|\langle y, \psi_{\bar{\mathbf{b}}, m} \rangle| \leq |\langle \gamma, \psi_{\bar{\mathbf{b}}, m} \rangle| + |\langle \eta, \psi_{\bar{\mathbf{b}}, m} \rangle| < h/2$. Then, we identify if $m \in \mathbb{S}_N$ by thresholding sequence $\langle y, \psi_{\bar{\mathbf{b}}, m} \rangle$ via the following inequalities.

$$\begin{cases} |\langle y, \psi_{\bar{\mathbf{b}}, m} \rangle| \geq h/2 & \text{if } m \in \mathbb{S}_N, \\ |\langle y, \psi_{\bar{\mathbf{b}}, m} \rangle| < h/2 & \text{otherwise,} \end{cases} \tag{95}$$

Sequence $\eta [\bar{\mathbf{k}}]$ is drawn from the normal distribution and is not bounded, therefore we can only guarantee that $|\langle \eta, \psi_{\bar{\mathbf{b}}, m} \rangle| < h/2 - (T_1 \Omega_1 e)^N \|f\|_\infty$ holds with a

given probability. However, we will show that modulo-hysteresis allows increasing this probability exponentially.

We use two properties of the p.d.f. of Gaussian distributions. First, given M random variables $\eta_i \sim \mathcal{N}(0, \sigma_i^2)$, $i = 1, \dots, M$ their summation satisfies $\sum_{i=1}^M \eta_i \sim \mathcal{N}(0, \sigma^2)$, where $\sigma = \sqrt{\sigma_1^2 + \dots + \sigma_M^2}$. Second, for a random variable $\eta_1 \sim \mathcal{N}(0, \sigma^2)$, the multiplication with a constant α yields $\alpha\eta_1 \sim \mathcal{N}(0, (\alpha\sigma)^2)$.

Then the noise term $\langle \eta, \psi_{\bar{\mathbf{b}}, m} \rangle$ satisfies

$$\begin{aligned} \langle \eta, \psi_{\bar{\mathbf{b}}, m} \rangle &= \sum_{\mathbf{k} \in \mathbb{Z}^{D-1}} \sum_{k_1 \in \mathbb{Z}} \frac{\Delta^N[k_1 - m] \cdot \eta[\mathbf{k}]}{N^B} \\ &= \sum_{k_1 \in \mathbb{Z}} \Delta^N[k_1 - m] \cdot \bar{\eta}[k_1], \quad \bar{\eta}[k_1] = \frac{1}{N^B} \sum_{\mathbf{k} \in \mathbb{Z}^{D-1}} \eta[\mathbf{k}]. \end{aligned} \quad (96)$$

Using the two p.d.f. properties above, $\bar{\eta} \sim \mathcal{N}\left(0, \left(\sigma\sqrt{N^B}/N^B\right)^2\right) = \mathcal{N}\left(0, \frac{\sigma^2}{N^B}\right)$. As expected, averaging gradually narrows down the p.d.f. of the distribution around the origin. Furthermore, we can write

$$\langle \eta, \psi_{\bar{\mathbf{b}}, m} \rangle = \Delta_-^N * \bar{\eta}[m], \quad \Delta_-^N[k_1] = \Delta^N[-k_1], \forall k_1 \in \mathbb{Z}. \quad (97)$$

Given that $\Delta_-^n = \Delta_-^1 * \dots * \Delta_-^{n-1}$, $\forall n \in \mathbb{Z}$, we will compute recursively the p.d.f. of $\langle \eta, \psi_{\bar{\mathbf{b}}, m} \rangle$ as follows. First, $\Delta_-^1 * \bar{\eta}[m] = \bar{\eta}[m+1] - \bar{\eta}[m]$. Given that $-\bar{\eta}[m] \sim \mathcal{N}\left(0, \frac{\sigma^2}{N^B}\right)$, we get $\Delta_-^1 * \bar{\eta}[m] \sim \mathcal{N}\left(0, \sigma^2 \frac{2}{N^B}\right)$. Recursively,

$$\Delta_-^N * \bar{\eta}[m] \sim \mathcal{N}\left(0, \sigma^2 \frac{2^N}{N^B}\right). \quad (98)$$

In the equation above one can notice that the finite difference degree N leads to an exponential increase in the standard deviation of the noise term. A very similar result was reported for bounded noise in the one-dimensional case [12, 14, 34]. However, in this multi-dimensional case we have the option to decrease the noise by increasing the number of samples $N^B = \prod_{d=2}^D \frac{B}{T_d}$. This can be done either by increasing the band size B within the allowable range ensuring $\mathcal{D}f < \min\{h/2, 2\lambda - 3h\}$, but also by decreasing the sampling periods T_d , $d = 2, \dots, D$. Both of these act only on dimensions x_2, \dots, x_D and are fully independent of dimension x_1 .

Therefore, the noise term $\langle \eta, \psi_{\bar{\mathbf{b}}, m} \rangle$ in (38) represents a random variable that allows to correctly evaluate if $m \in \mathbb{S}_N$ via (95) when $\langle \eta, \psi_{\bar{\mathbf{b}}, m} \rangle < h/2 - (T_1 \Omega_1 e)^N \|f\|_\infty$.

The probability that this doesn't hold is denoted by p_{err} which is calculated using the p.d.f. of the normal distribution as

$$p_{\text{err}} = 2 \int_{\eta_{\text{max}}}^{\infty} \frac{1}{\sigma_0 \sqrt{2\pi}} \cdot e^{-\frac{1}{2} \left(\frac{x}{\sigma_0} \right)^2} dx, \quad (99)$$

where $\sigma_0 = \sigma \cdot \sqrt{\frac{2^N}{N^B}}$ and $\eta_{\text{max}} = h/2 - (T_1 \Omega_1 e)^N \|f\|_{\infty}$. The integral above can be bounded in terms of the *complementary error function* as follows, which finalizes the proof [38, 39]

$$p_{\text{err}} \leq e^{-\left(\frac{\eta_{\text{max}}}{\sigma_0 \sqrt{2}} \right)^2}. \quad (100)$$

□

Proof for Proposition 7 (Detection of constants $M_{\bar{\mathbf{b}}}$). We define by $y_{\bar{\mathbf{b}}, \bar{\mathbf{b}}^*}$ the samples y filtered with $\psi_{\bar{\mathbf{b}}, \bar{\mathbf{b}}^*}$ where $\bar{\mathbf{b}}^* \in \text{Neighbors}(\bar{\mathbf{b}})$, such that $[\bar{\mathbf{b}}^*]_{d^*} = [\bar{\mathbf{b}}]_{d^*} + 1$ and

$$y_{\bar{\mathbf{b}}, \bar{\mathbf{b}}^*} = \langle y, \psi_{\bar{\mathbf{b}}, \bar{\mathbf{b}}^*} \rangle = \langle \gamma, \psi_{\bar{\mathbf{b}}, \bar{\mathbf{b}}^*} \rangle - \langle \varepsilon_{\gamma}, \psi_{\bar{\mathbf{b}}, \bar{\mathbf{b}}^*} \rangle + \langle \eta, \psi_{\bar{\mathbf{b}}, \bar{\mathbf{b}}^*} \rangle$$

Along the same lines as (91), we derive

$$|\langle \gamma, \psi_{\bar{\mathbf{b}}, \bar{\mathbf{b}}^*} \rangle| \leq (T_{d^*} \Omega_{d^*} e)^N \|f\|_{\infty}. \quad (101)$$

Along dimension x_{d^*} and for $\bar{\mathbf{T}}\bar{\mathbf{k}} \in \mathcal{R}_{\bar{\mathbf{b}}} \cup \mathcal{R}_{\bar{\mathbf{b}}^*}$, $k_1 = 0$, the support of $\psi_{\bar{\mathbf{b}}, \bar{\mathbf{b}}^*}$ is

$$\{N_{d^*}^B [\bar{\mathbf{b}}^*]_{d^*} - 1, \dots, N_{d^*}^B [\bar{\mathbf{b}}^*]_{d^*} - 1 + N\}.$$

Furthermore, the discontinuity between the bands would be located in between the samples $(N_{d^*}^B [\bar{\mathbf{b}}^*]_{d^*} - 1) T_{d^*}$, $N_{d^*}^B [\bar{\mathbf{b}}^*]_{d^*} T_{d^*}$. Using the same reasoning as before (92-93)

$$\begin{cases} |\langle \varepsilon_{\gamma}, \psi_{\bar{\mathbf{b}}, \bar{\mathbf{b}}^*} \rangle| \geq h & \text{if } M_{\bar{\mathbf{b}}} \neq M_{\bar{\mathbf{b}}^*}, \\ |\langle \varepsilon_{\gamma}, \psi_{\bar{\mathbf{b}}, \bar{\mathbf{b}}^*} \rangle| = 0 & \text{otherwise,} \end{cases} \quad (102)$$

Therefore, if $(T_{d^*} \Omega_{d^*} e)^N \|f\|_{\infty} < h/2$ and $|\langle \eta, \psi_{\bar{\mathbf{b}}, \bar{\mathbf{b}}^*} \rangle| < h/2 - (T_{d^*} \Omega_{d^*} e)^N \|f\|_{\infty}$, then, if $M_{\bar{\mathbf{b}}} \neq M_{\bar{\mathbf{b}}^*}$, as before, we get (94)

$$|\langle y, \psi_{\bar{\mathbf{b}}, \bar{\mathbf{b}}^*} \rangle| \geq h/2.$$

Therefore, as before (95), we identify if $M_{\bar{\mathbf{b}}} \neq M_{\bar{\mathbf{b}}^*}$ by thresholding sequence $\langle y, \psi_{\bar{\mathbf{b}}, \bar{\mathbf{b}}^*} \rangle$ via the following inequalities:

$$\begin{cases} |\langle y, \psi_{\bar{\mathbf{b}}, \bar{\mathbf{b}}^*} \rangle| \geq h/2 & \text{if } M_{\bar{\mathbf{b}}} \neq M_{\bar{\mathbf{b}}^*}, \\ |\langle y, \psi_{\bar{\mathbf{b}}, \bar{\mathbf{b}}^*} \rangle| < h/2 & \text{otherwise.} \end{cases} \quad (103)$$

Assuming that $M_{\bar{\mathbf{b}}} \neq M_{\bar{\mathbf{b}}^*}$, we compute $\text{sign}(\langle y, \psi_{\bar{\mathbf{b}}, \bar{\mathbf{b}}^*} \rangle)$ as follows. We first show that

$$\text{sign}(\langle y, \psi_{\bar{\mathbf{b}}, \bar{\mathbf{b}}^*} \rangle) = -\text{sign}(\langle \varepsilon_\gamma, \psi_{\bar{\mathbf{b}}, \bar{\mathbf{b}}^*} \rangle) \quad (104)$$

If we assume by contradiction that $\text{sign}(\langle y, \psi_{\bar{\mathbf{b}}, \bar{\mathbf{b}}^*} \rangle) = \text{sign}(\langle \varepsilon_\gamma, \psi_{\bar{\mathbf{b}}, \bar{\mathbf{b}}^*} \rangle)$ we get $|\langle y, \psi_{\bar{\mathbf{b}}, \bar{\mathbf{b}}^*} \rangle + \langle \varepsilon_\gamma, \psi_{\bar{\mathbf{b}}, \bar{\mathbf{b}}^*} \rangle| = |\langle \gamma, \psi_{\bar{\mathbf{b}}, \bar{\mathbf{b}}^*} \rangle| < h/2$. However, from (102)-(103) we have that $|\langle y, \psi_{\bar{\mathbf{b}}, \bar{\mathbf{b}}^*} \rangle| \geq h/2$ and $|\langle \varepsilon_\gamma, \psi_{\bar{\mathbf{b}}, \bar{\mathbf{b}}^*} \rangle| > 0$. Given our assumption that the two quantities have the same sign, we get a contradiction and thus (104) is true.

Using the expression of $\psi_{\bar{\mathbf{b}}, \bar{\mathbf{b}}^*}$ in (37), the definition of the residual in (20) and Proposition 5, it can be shown directly that

$$\langle \varepsilon_\gamma, \psi_{\bar{\mathbf{b}}, \bar{\mathbf{b}}^*} \rangle = h(M_{\bar{\mathbf{b}}^*} - M_{\bar{\mathbf{b}}})(-1)^{N+1} \Rightarrow \text{sign}(\langle \varepsilon_\gamma, \psi_{\bar{\mathbf{b}}, \bar{\mathbf{b}}^*} \rangle) = (M_{\bar{\mathbf{b}}^*} - M_{\bar{\mathbf{b}}})(-1)^{N+1},$$

and thus $\text{sign}(\langle y, \psi_{\bar{\mathbf{b}}, \bar{\mathbf{b}}^*} \rangle) = (M_{\bar{\mathbf{b}}^*} - M_{\bar{\mathbf{b}}})(-1)^N$. Finally, we get that

$$\begin{cases} M_{\bar{\mathbf{b}}^*} = M_{\bar{\mathbf{b}}} + \text{sign}(\langle y, \psi_{\bar{\mathbf{b}}, \bar{\mathbf{b}}^*} \rangle) (-1)^N & \text{if } |\langle y, \psi_{\bar{\mathbf{b}}, \bar{\mathbf{b}}^*} \rangle| \geq h/2, \\ M_{\bar{\mathbf{b}}^*} = M_{\bar{\mathbf{b}}} & \text{otherwise.} \end{cases} \quad (105)$$

Furthermore, the filtered noise satisfies (96-98)

$$\langle \eta, \psi_{\bar{\mathbf{b}}, \bar{\mathbf{b}}^*} \rangle \sim \mathcal{N}\left(0, \sigma^2 \frac{2^N}{N^{B^*}}\right). \quad (106)$$

Then, the probability that $|\langle \eta, \psi_{\bar{\mathbf{b}}, \bar{\mathbf{b}}^*} \rangle| < h/2 - (T_{d^*} \Omega_{d^*} e)^N \|f\|_\infty$ doesn't hold, denoted by p_{err} , satisfies

$$p_{\text{err}} \leq e^{-\left(\frac{\eta_{\max}}{\sigma_0 \sqrt{2}}\right)^2}. \quad (107)$$

where $\sigma_0 = \sigma \cdot \sqrt{\frac{2^N}{N^{B^*}}}$ and $\eta_{\max} = h/2 - (T_{d^*} \Omega_{d^*} e)^N \|f\|_\infty$. \square

Proof for Theorem 2 (Noiseless input recovery). We note that, for $\sigma \rightarrow 0$, the results in Proposition 6 and 7 hold true with probability 1. We then compute $\widetilde{M}_{\bar{\mathbf{b}}}$ using

Proposition 7 as follows. Given that $\widetilde{M}_0 = 0$ by definition, one can compute successively $\widetilde{M}_{[b_2, 0, \dots, 0]}$ from $\widetilde{M}_{[b_2-1, 0, \dots, 0]}$ for $\forall b_2 \in \mathbb{Z}_+$ and subsequently $\widetilde{M}_{[b_2, 0, \dots, 0]}$ from $\widetilde{M}_{[b_2+1, 0, \dots, 0]}$ for $\forall b_2 \in \mathbb{Z}_-$. Repeating the process for $b_d, d \in \{3, \dots, D\}$ yields $\widetilde{M}_{\bar{\mathbf{b}}}, \forall \bar{\mathbf{b}} \in \mathbb{Z}^{D-1}$.

To compute the folding times via Proposition 6, we require that the sets characterized by each folding time in \mathbb{S}_N do not overlap. Specifically we require that

$$\left\{ \left[\frac{\tau_{\bar{\mathbf{b}}, r_1}}{T_1} \right] - N, \dots, \left[\frac{\tau_{\bar{\mathbf{b}}, r_1}}{T_1} \right] \right\} \cap \left\{ \left[\frac{\tau_{\bar{\mathbf{b}}, r_2}}{T_1} \right] - N, \dots, \left[\frac{\tau_{\bar{\mathbf{b}}, r_2}}{T_1} \right] \right\} = \emptyset,$$

for $\forall r_1, r_2 \in \mathbb{Z}, r_1 \neq r_2$. A sufficient condition for this is

$$\left[\frac{\tau_{\bar{\mathbf{b}}, r_2}}{T_1} \right] - N - \left[\frac{\tau_{\bar{\mathbf{b}}, r_1}}{T_1} \right] > \frac{\tau_{\bar{\mathbf{b}}, r_2}}{T_1} - \frac{\tau_{\bar{\mathbf{b}}, r_1}}{T_1} - (N + 1) > 0, \quad (108)$$

which can be guaranteed via Proposition 2 if

$$(N + 1) T_1 < \frac{h}{\Omega_1 \|f\|_\infty}. \quad (109)$$

Without reducing the generality we first assume that $x_1 \geq 0$ and thus $r, k_1 \geq 0$. As before, the case $x_1 \leq 0$ is treated as a mirrored version of $x_1 \geq 0$. An immediate consequence of (108) is that for $r_1 = 0, r_2 = 1 \Rightarrow \left[\frac{\tau_{\bar{\mathbf{b}}, 1}}{T_1} \right] \geq N + 1$. Because there is no actual jump taking place at $\tau_{\bar{\mathbf{b}}, 0} = 0 \Rightarrow |\langle \varepsilon_\gamma, \psi_{\bar{\mathbf{b}}, 0} \rangle| = 0$ and $|\langle y, \psi_{\bar{\mathbf{b}}, 0} \rangle| < h/2$ via Proposition 6. The smallest m for which filtered output satisfies $|\langle y, \psi_{\bar{\mathbf{b}}, m} \rangle| \geq h/2$ is $m = m_{\min}^1 \triangleq \left[\frac{\tau_{\bar{\mathbf{b}}, 1}}{T_1} \right] - N$. The last index m corresponding to folding time $\tau_{\bar{\mathbf{b}}, 1}$ detected via $|\langle y, \psi_{\bar{\mathbf{b}}, m} \rangle| \geq h/2$ is $m = m_{\max}^1 \triangleq \left[\frac{\tau_{\bar{\mathbf{b}}, 1}}{T_1} \right]$. We can compute m_{\min}^1 and m_{\max}^1 as

$$m_{\min}^1 = \min \{ m > 0 \mid |\langle y, \psi_{\bar{\mathbf{b}}, m} \rangle| \geq h/2 \}, \quad (110)$$

$$m_{\max}^1 = m_{\min}^1 + N. \quad (111)$$

Assuming (109) to be true, one can then compute recursively sequences m_{\min}^r, m_{\max}^r corresponding to folding time $\tau_{\bar{\mathbf{b}}, r}$ as follows

$$m_{\min}^r = \min \{ m > m_{\min}^{r-1} + N \mid |\langle y, \psi_{\bar{\mathbf{b}}, m} \rangle| \geq h/2 \}, \quad (112)$$

$$m_{\max}^r = m_{\min}^r + N. \quad (113)$$

The folding time is estimated as $\tilde{\tau}_{\bar{\mathbf{b}},r} = [m_{\min}^r + N] \cdot T_1$. As in the case $r = 1$ we can show that $m_{\min}^r = \left\lceil \frac{\tau_{\bar{\mathbf{b}},r}}{T_1} \right\rceil - N$. Therefore $\tilde{\tau}_{\bar{\mathbf{b}},r} = \left\lceil \frac{\tau_{\bar{\mathbf{b}},r}}{T_1} \right\rceil \cdot T_1$. Even though the folding time is not perfectly computed, this has no effect on the input recovery because $\left\lceil \frac{\tilde{\tau}_{\bar{\mathbf{b}},r}}{T_1} \right\rceil = \left\lceil \frac{\tau_{\bar{\mathbf{b}},r}}{T_1} \right\rceil$ and we only evaluate the residual at the sampling locations $\mathbf{k}\mathbf{T}$. This means that replacing $\tau_{\bar{\mathbf{b}},r}$ by $\left\lceil \frac{\tau_{\bar{\mathbf{b}},r}}{T_1} \right\rceil \cdot T_1$ in the expression of $\varepsilon_f(\mathbf{V}\mathbf{T}\mathbf{k})$ yields the same values (see Definition 2)

$$\begin{aligned} \varepsilon_\gamma[\mathbf{k}] &= h \left[M_{\bar{\mathbf{b}}} + \sum_{i=0}^r s_{\bar{\mathbf{b}},r} \mathbb{1}_{[\tau_{\bar{\mathbf{b}},r}, \infty)}(k_1 T_1) \right] \\ &= h \left[M_{\bar{\mathbf{b}}} + \sum_{i=0}^r s_{\bar{\mathbf{b}},r} \mathbb{1}_{\left[\left\lceil \frac{\tau_{\bar{\mathbf{b}},r}}{T_1} \right\rceil \cdot T_1, \infty\right)}(k_1 T_1) \right]. \end{aligned} \quad (114)$$

We note that, as explained before, we do not recover $M_{\bar{\mathbf{b}}}$ but $\widetilde{M}_{\bar{\mathbf{b}}} = M_{\bar{\mathbf{b}}} - M_{\bar{\mathbf{0}}}$. This will be accounted for at the final input reconstruction stage.

Furthermore, we estimate the sign as $\tilde{s}_{\bar{\mathbf{b}},r} = -\text{sign} \langle y, \psi_{\bar{\mathbf{b}}, m_{\min}^r} \rangle$. We will show that $\tilde{s}_{\bar{\mathbf{b}},r} = s_{\bar{\mathbf{b}},r}$ as follows. Given that $|\langle \gamma, \psi_{\bar{\mathbf{b}}, m_{\min}^r} \rangle| < h/2$ and $|\langle y, \psi_{\bar{\mathbf{b}}, m_{\min}^r} \rangle| \geq h/2$, then, via (38), it follows that

$$\text{sign} \langle y, \psi_{\bar{\mathbf{b}}, m_{\min}^r} \rangle = -\text{sign} \langle \varepsilon_\gamma, \psi_{\bar{\mathbf{b}}, m_{\min}^r} \rangle.$$

We use the fact that $\varepsilon_\gamma[\mathbf{k}]$ does not change for $\bar{\mathbf{k}}\bar{\mathbf{T}} \in \mathcal{R}_{\bar{\mathbf{b}}}$. For $N \geq 1$, using the expression of Δ^N and (114),

$$\begin{aligned} \langle \varepsilon_\gamma, \psi_{\bar{\mathbf{b}}, m_{\min}^r} \rangle &= \langle \varepsilon_\gamma, \Delta^N [\cdot - m_{\min}^r] \rangle \\ &= h s_{\bar{\mathbf{b}},r} \sum_{k_1 \in \mathbb{Z}} \mathbb{1}_{\left[\left\lceil \frac{\tau_{\bar{\mathbf{b}},r}}{T_1} \right\rceil \cdot T_1, \infty\right)}(k_1 T_1) \cdot \Delta^N [k_1 - m_{\min}^r] \\ &= h s_{\bar{\mathbf{b}},r} \sum_{k_1 \in \mathbb{Z}} \mathbb{1}_{\left[(m_{\min}^r + N) \cdot T_1, \infty\right)}(k_1 T_1) \cdot \Delta^N [k_1 - m_{\min}^r] \end{aligned} \quad (115)$$

By applying the change of variable $k_1^* = k_1 - m_{\min}^r - N$

$$\langle \varepsilon_\gamma, \psi_{\bar{\mathbf{b}}, m_{\min}^r} \rangle = h s_{\bar{\mathbf{b}},r} \sum_{k_1^* \in \mathbb{Z}} \mathbb{1}_{[0, \infty)}(k_1^* T_1) \cdot \Delta^N [k_1^* + N] \quad (116)$$

$$= h s_{\bar{\mathbf{b}},r} \sum_{k_1^* \in \mathbb{Z}_+} \Delta^N [k_1^* + N] = h s_{\bar{\mathbf{b}},r}. \quad (117)$$

The last equality can be shown recursively via direct calculation for $N \geq 1$, given that $k_1 \geq 0$, which proves that $s_{\bar{\mathbf{b}},r} = \tilde{s}_{\bar{\mathbf{b}},r}$.

After the folding times and signs are computed as above for all $\bar{\mathbf{b}} \in \mathbb{Z}^{D-1}$, the input samples are reconstructed as

$$\tilde{\gamma}[\mathbf{k}] = y[\mathbf{k}] + \tilde{\varepsilon}_\gamma[\mathbf{k}], \quad (118)$$

where $\tilde{\varepsilon}_\gamma[\mathbf{k}] = h \left[\widetilde{M}_{\bar{\mathbf{b}}} + \sum_{i=0}^r s_{\bar{\mathbf{b}},r} \mathbb{1}_{[\tau_{\bar{\mathbf{b}},r}, \infty)}(k_1 T_1) \right] = \varepsilon_\gamma[\mathbf{k}] - hM_{\bar{\mathbf{0}}}$, which leads to $\tilde{\gamma}[\mathbf{k}] = \gamma[\mathbf{k}] - hM_{\bar{\mathbf{0}}}$. \square

8. Conclusion

The Unlimited Sampling Framework (USF) provides sampling rate guarantees that allow tackling high dynamic range signals in the one-dimensional case. For multi-dimensional signals, USF is typically applied sequentially, thus not exploiting the multi-dimensional structure of the input. In this paper, we

- introduced the first multi-dimensional modulo operator and associated input reconstruction method from lattice samples,
- derived sampling rate conditions under which the reconstruction is perfect in the noiseless scenario,
- provided probability error bounds under Gaussian noise assumption,
- showed numerically that, while USF does not allow noise amplitudes larger than the modulo threshold, the proposed approach allows arbitrarily high noise for sufficiently small sampling times.

This work can be extended in a number of ways

1. It can be coupled with modulo denoising approaches such as [31] to yield enhanced reconstruction algorithms.
2. While it is assumed that the input is bandlimited, this work can be extended for inputs generated with B-splines or sparse inputs.
3. The model in our work can be extended to a wider range of models such as modulo neuromorphic architectures, that could exploit multi-dimensional inputs in a similar way to the biological systems [40] [24].

4. Alternative sampling mechanisms that would benefit from a multi-dimensional modulo operation include one-bit sampling [41] or average sampling [33].
5. The current line of work can lead to a the implementation of a new multi-dimensional hardware prototype.

References

- [1] R. M. Gray, D. L. Neuhoff, Quantization, *IEEE Trans. Inf. Theory* 44 (6) (1998) 2325–2383. doi:10.1109/18.720541.
- [2] W. Sun, X. Zhou, Reconstruction of band-limited functions from local averages, *Constructive Approximation* 18 (2) (2002) 205–222. doi:10.1007/s00365-001-0011-y.
- [3] D. L. Donoho, I. M. Johnstone, Ideal spatial adaptation by wavelet shrinkage, *Biometrika* 81 (3) (1994) 425–455. doi:10.1093/biomet/81.3.425.
- [4] T. Blumensath, M. E. Davies, Iterative hard thresholding for compressed sensing, *Applied and Computational Harmonic Analysis* 27 (3) (2009) 265–274. doi:10.1016/j.acha.2009.04.002.
- [5] B. Smith, Instantaneous companding of quantized signals, *The Bell System Technical Journal* 36 (3) (1957) 653–710. doi:10.1002/j.1538-7305.1957.tb03858.x.
- [6] P. Smaragdis, Dynamic range extension using interleaved gains, *IEEE Audio, Speech, Language Process.* 17 (5) (2009) 966–973. doi:10.1109/tasl.2008.2012322.
URL <http://dx.doi.org/10.1109/TASL.2008.2012322>
- [7] J. Abel, J. Smith, Restoring a clipped signal, in: *IEEE Intl. Conf. on Acoustics, Speech and Sig. Proc. (ICASSP)*, 1991. doi:10.1109/icassp.1991.150655.
URL <http://dx.doi.org/10.1109/icassp.1991.150655>

- [8] J. Zhang, J. Hao, X. Zhao, S. Wang, L. Zhao, W. Wang, Z. Yao, Restoration of clipped seismic waveforms using projection onto convex sets method, *Nature Sci. Rep.* 6 (1). doi:10.1038/srep39056.
URL <https://doi.org/10.1038/srep39056>
- [9] A. Adler, V. Emiya, M. G. Jafari, M. Elad, R. Gribonval, M. D. Plumbley, Audio inpainting, *IEEE Trans. Acoust., Speech, Signal Process.* 20 (3) (2012) 922–932. doi:10.1109/tasl.2011.2168211.
URL <https://doi.org/10.1109/tasl.2011.2168211>
- [10] P. E. Debevec, J. Malik, Recovering high dynamic range radiance maps from photographs, in: *ACM Siggraph*, 1997. doi:10.1145/258734.258884.
URL <https://doi.org/10.1145/258734.258884>
- [11] A. Bhandari, F. Krahmer, R. Raskar, On unlimited sampling, in: *Intl. Conf. on Sampling Theory and Applications (SampTA)*, 2017, pp. 31–35. doi:10.1109/sampta.2017.8024471.
URL <https://doi.org/10.1109/sampta.2017.8024471>
- [12] A. Bhandari, F. Krahmer, R. Raskar, On unlimited sampling and reconstruction, *IEEE Trans. Sig. Proc.* 69 (2020) 3827–3839. doi:10.1109/tsp.2020.3041955.
- [13] A. Bhandari, F. Krahmer, T. Poskitt, Unlimited sampling from theory to practice: Fourier-Prony recovery and prototype ADC, *IEEE Trans. Sig. Proc.* (2021) 1131–1141 doi:10.1109/TSP.2021.3113497.
- [14] D. Florescu, F. Krahmer, A. Bhandari, The surprising benefits of hysteresis in unlimited sampling: Theory, algorithms and experiments, *IEEE Trans. Sig. Proc.* 70 (2022) 616–630. doi:10.1109/tsp.2022.3142507.
- [15] A. Bhandari, F. Krahmer, R. Raskar, Unlimited sampling of sparse signals, in: *IEEE Intl. Conf. on Acoustics, Speech and Signal Processing (ICASSP)*, 2018, pp. 4569–4573. doi:10.1109/icassp.2018.8462231.

- [16] A. Bhandari, F. Krahmer, R. Raskar, Unlimited sampling of sparse sinusoidal mixtures, in: *IEEE Intl. Sym. on Information Theory (ISIT)*, 2018, pp. 336–340. doi:10.1109/isit.2018.8437122.
- [17] A. Bhandari, F. Krahmer, On identifiability in unlimited sampling, in: *Intl. Conf. on Sampling Theory and Applications (SampTA)*, 2019.
- [18] A. Bhandari, F. Krahmer, R. Raskar, Methods and apparatus for modulo sampling and recovery (May 2020).
- [19] A. Bhandari, F. Krahmer, HDR imaging from quantization noise, in: *IEEE Intl. Conf. on Image Processing (ICIP)*, 2020, pp. 101–105. doi:10.1109/icip40778.2020.9190872.
- [20] V. Shah, C. Hegde, Signal reconstruction from modulo observations, in: *2019 IEEE Global Conference on Signal and Information Processing (GlobalSIP)*, IEEE, 2019, pp. 1–5.
- [21] O. Musa, P. Jung, N. Goertz, Generalized approximate message passing for unlimited sampling of sparse signals, in: *IEEE Global Conf. on Signal and Information Proc.*, 2018, pp. 336–340.
- [22] S. Rudresh, A. Adiga, B. A. Shenoy, C. S. Seelamantula, Wavelet-based reconstruction for unlimited sampling, in: *IEEE Intl. Conf. on Acoustics, Speech and Signal Processing (ICASSP)*, 2018, pp. 4584–4588.
- [23] A. Bhandari, Back in the US-SR: Unlimited sampling and sparse super-resolution with its hardware validation, *IEEE Signal Process. Lett.* 29 (2022) 1047 – 1051.
- [24] D. Florescu, F. Krahmer, A. Bhandari, Event-driven modulo sampling, in: *IEEE Intl. Conf. on Acoustics, Speech and Signal Processing (ICASSP)*, 2021, pp. 5435–5439. doi:10.1109/icassp39728.2021.9414152.
- [25] D. Florescu, A. Bhandari, Modulo event-driven sampling: System identification and hardware experiments, in: *IEEE Intl. Conf. on Acoustics, Speech and Signal Processing (ICASSP)*, 2022, pp. 5747–5751.

- [26] M. Beckmann, A. Bhandari, F. Krahmer, The modulo Radon transform: Theory, algorithms, and applications, *SIAM Journal on Imaging Sciences* 15 (2) (2022) 455–490. doi:10.1137/21m1424615.
- [27] S. Fernandez-Menduina, F. Krahmer, G. Leus, A. Bhandari, Computational array signal processing via modulo non-linearities, *IEEE Trans. Sig. Proc.* 70 (2022) 2168–2179.
- [28] V. Bouis, F. Krahmer, A. Bhandari, Multidimensional unlimited sampling: A geometrical perspective, in: *European Sig. Proc. Conf. (EUSIPCO)*, 2020, pp. 2314–2318.
- [29] X. Zhao, J. Chen, M. Karczewicz, A. Said, V. Seregin, Joint separable and non-separable transforms for next-generation video coding, *IEEE Trans. Image Proc.* 27 (5) (2018) 2514–2525.
- [30] A. Cohen, I. Daubechies, Non-separable bidimensional wavelet bases, *Revista Matematica Iberoamericana* 9 (1) (1993) 51–137.
- [31] H. Tyagi, Error analysis for denoising smooth modulo signals on a graph, *Applied and Computational Harmonic Analysis* 57 (2022) 151–184.
- [32] M. Fanuel, H. Tyagi, Denoising modulo samples: k-nn regression and tightness of sdp relaxation, *Information and Inference: A Journal of the IMA* 11 (2) (2022) 637–677.
- [33] D. Florescu, A. Bhandari, Unlimited sampling with local averages, in: *IEEE Intl. Conf. on Acoustics, Speech and Signal Processing (ICASSP)*, 2022, pp. 5742–5746.
- [34] D. Florescu, A. Bhandari, Unlimited sampling via generalized thresholding, in: *IEEE Intl. Symp. on Information Theory (ISIT)*, 2022, pp. 1606–1611.
- [35] D. Florescu, F. Krahmer, A. Bhandari, Unlimited sampling with hysteresis, in: *55th Asilomar Conf. on Signals, Systems, and Computers*, 2021, pp. 831–835. doi:10.1109/ieeeeconf53345.2021.9723306.

- [36] E. Viscito, J. P. Allebach, The analysis and design of multidimensional FIR perfect reconstruction filter banks for arbitrary sampling lattices, *IEEE Trans. Circuits Syst.* 38 (1) (1991) 29–41.
- [37] Y. M. Lu, M. N. Do, R. S. Laugesen, A computable Fourier condition generating alias-free sampling lattices, *IEEE Trans. Sig. Proc.* 57 (5) (2009) 1768–1782.
- [38] M. Chiani, D. Dardari, M. K. Simon, New exponential bounds and approximations for the computation of error probability in fading channels, *IEEE Trans. Wireless Commun.* 2 (4) (2003) 840–845.
- [39] J. Wozencraft, I. M. Jacobs, *Principles of communication engineering.*, Wiley, 1965.
- [40] G. Gallego, T. Delbrück, G. Orchard, C. Bartolozzi, B. Taba, A. Censi, S. Leutenegger, A. J. Davison, J. Conradt, K. Daniilidis, et al., Event-based vision: A survey, *IEEE Trans. Pattern Anal. Mach. Intell.* 44 (1) (2020) 154–180.
- [41] O. Graf, A. Bhandari, F. Kraemer, One-bit unlimited sampling, in: *IEEE Intl. Conf. on Acoustics, Speech and Signal Processing (ICASSP)*, 2019, pp. 5102–5106.